Environmental Science and Pollution Research (2021) 28:52046–52063
https://doi.org/10.1007/s11356-021-14427-y

RESEARCH ARTICLE

Nanoencapsulation of thyme essential oil: a new avenue to enhance its protective role against oxidative stress and cytotoxicity of zinc oxide nanoparticles in rats

Marwa E. Hassan[1] · Rasha R. Hassan[2] · Kawthar A. Diab[3] · Aziza A. El-Nekeety[4] · Nabila S. Hassan[5] · Mosaad A. Abdel-Wahhab[4]

Received: 17 January 2021 / Accepted: 10 May 2021 / Published online: 17 May 2021

Abstract

Although the green synthesis of nanometals is eco-friendly, the toxicity or safety of these biosynthesized nanoparticles in living organisms is not fully studied. This study aimed to evaluate the potential protective role of encapsulated thyme oil (ETO) against zinc oxide nanoparticles (ZnO-NPs). ETO was prepared using a mixture of whey protein isolate, maltodextrin, and gum Arabic, and ZnO-NPs were synthesized using parsley extract. Six groups of male Sprague-Dawley rats were treated orally for 21 days which included the control group, ZnO-NP-treated group (25 mg/kg body weight (b.w.)), ETO-treated groups at low or high dose (50, 100 mg/kg b.w.), and the groups that received ZnO-NPs plus ETO at the two tested doses. Blood and tissue samples were collected for different assays. The results showed that carvacrol and thymol were the major components in ETO among 13 compounds isolated by GC-MS. ZnO-NPs were nearly spherical and ETOs were round in shape with an average size of 38 and 311.8 nm, respectively. Administration of ZnO-NPs induced oxidative stress, DNA damage, biochemical, ctyogentical, and histological changes in rats. ETO at the tested doses alleviated these disturbances and showed protective effects against the hazards of ZnO-NPs. It could be concluded that encapsulation of thyme oil using whey protein isolate, maltodextrin, and gum Arabic improved the antioxidant properties of ETO, probably possess synergistic effects, and can be used as a promising tool in pharmaceutical and food applications.

Keywords Zinc oxide nanoparticles · Encapsulated thyme essential oil · Oxidative stress · Cytotoxicity · Nanotechnology · Antioxidant

Introduction

In recent years, nanotechnology has been utilized in food industries as a tool to produce healthier, safer, and better-tasting food resulting in the development of a novel category of food named nanofood (Wang et al. 2014a) and as delivery systems for drug (Zahin et al. 2020). It is used to improve antimicrobial packaging through the incorporation of some active components that can deliver functional attributes to traditional active packaging (Müller and Schmid 2019). However, the interactions of the biological systems with nanoparticles have several unpredictable outcomes; hence, the understanding of their toxicity is very essential to protect the human body from their hazardous effects (John et al. 2010; Rasmussen et al. 2010; Sharma et al. 2011). Consequently, in the year 2011, the European Parliament called for additional checks of sufficient safety assessment of the nanofood and requested that all nanofood should be labeled (Wang et al. 2014a). Unfortunately, most of the markets unintentionally or intentionally did not follow these new rules, and until now there are no specific labels to indicate if the food contains nanomaterials. Moreover, most of the methods used for nanomaterial fabrication are not environmentally friendly;

Responsible Editor: Mohamed M. Abdel-Daim

✉ Mosaad A. Abdel-Wahhab
mosaad_abdelwahhab@yahoo.com

[1] Toxicology Department, Research Institute of Medical Entomology, Cairo, Egypt

[2] Immunology Department, Research Institute of Medical Entomology, Cairo, Egypt

[3] Genetics and Cytology Department, National Research Center, Dokki, Cairo, Egypt

[4] Food Toxicology & Contaminants Department, National Research Center, Dokki, Cairo, Egypt

[5] Pathology Department, National Research Center, Dokki, Cairo, Egypt

hence, the use of eco-friendly green approaches for the synthesis of nanoparticles was recently developed. The most developed green methods of nanoparticle fabrication using plant extracts, fungi, algae, and bacteria were reviewed recently by El-Seedi et al. (2019) and Hamida et al. (2020). Several metal nanoparticles were successfully synthesized using these approaches including silver nanoparticles (Bin-Meferij and Hamida 2019) and ZnO-NPs (Lakshmi et al. 2017).

ZnO-NPs are used excessively in biomedical applications such as a tool for the imaging of biological systems, cosmetics, and anticancer drugs (Jiang et al. 2018). Moreover, Zn is used as a food supplement particularly for children (Pourmirzaiee et al. 2018; Prasad 2008) and currently during the COVID-19 pandemic (Wessels et al. 2020) besides the wide use of ZnO-NPs for longer preservations and extend shelf life of several foods (Wu et al. 2010; Espitia et al. 2012). Despite these beneficial effects of ZnO-NPs, several studies reported that ZnO-NPs produce cytotoxicity in different cell types such as osteoblast cancer cells, kidney cells, hepatocytes, human bronchial epithelial cells, and alveolar adenocarcinoma cells and the toxicity of such nanoparticles may be correlated to the dosage and the size of nanoparticles (Singh 2019; Wang et al. 2018). Exposure to ZnO-NPs led to cytotoxicity in a time- and dose-dependent as a consequence of the oxidative stress, the peroxidation of lipids, the damage of carbohydrates, proteins, cell membrane, and DNA (Almansour et al. 2017; Fadoju et al. 2019). Additionally, because of the high solubility, ZnO-NPs can exist at high concentrations to produce oxidative stress, cytotoxicity, and mitochondrial dysfunction (Wang et al. 2019; Yan et al. 2020).

Thyme (*Thymus vulgaris*) is an herb widely used as species in human food and has received huge concern because of its beneficial additives in nutrition (Hesabi Nameghi et al. 2019). It has a beneficial role on the health and improves the appetite and the secretion of the endogenous enzyme, and activates the immune responses along with its role as an antioxidant, anthelminthic, and antiviral properties (El-Nekeety et al. 2011; Toujani et al. 2018), whereas some characteristics of the bioactive compounds in the essential oil of thyme especially the high activity, hydrophobia, reactivity, sensitivity to peroxidation, and volatility caused limitations in its use in some foods (Hossain et al. 2019). Consequently, its efficiency and sensory quality probably decreased due to these undesirable reactions resulting in the decrease of palatability if used in high amounts (Lee et al. 2004). The use of encapsulation technique is an attractive tool to protect these active components in the essential oils and also to improve their delivery and controlled release via the entrapment in the core of the nano-capsule structure of membrane wall and/or the adsorption onto the carrier (Abdel-Wahhab et al. 2018). This study was conducted to use whey protein isolate-maltodextrin gum Arabic for the synthesis of encapsulated thyme essential oil and to evaluate their efficiency to counteract the oxidative stress and cytogenetic toxicity of ZnO-NPs in rats.

Materials and methods

Chemicals and kits

Zinc acetate dehydrates, maltodextrin (MD), and whey protein isolate (WPI) were purchased from Sigma-Aldrich (St. Louis, USA); however, gum Arabic (GA) was provided by San-Ei Gen F.F.I. Inc. (Osaka, Japan). Kits for transaminase (ALT and AST), cholesterol (Cho), triglycerides (TriG), high-density lipoprotein (HDL), low-density lipoprotein (LDL), creatinine, urea, albumin (Alb), and total protein (TP) were obtained from FAR Diagnostics Co. (Via Fermi, Italy). Kits for catalase (CAT), nitric oxide (NO), superoxide dismutase (SOD), and total antioxidants capacity (TAC) were obtained from Eagle diagnostics (Dallas, TX, USA). Malondialdehyde (MDA) was obtained from Oxis Research TM Co. (USA). ELISA kit for alpha-fetoprotein (AFP) was purchased from Biochem Immuno Systems Co. (Montreal, Canada). A tumor necrosis factor-alpha (TNF-α) kit was purchased from Orgenium (Helsinki, Finland). A kit for measuring carcinoembryonic antigen (CEA) was obtained from Biodiagnostic (Giza, Egypt).

Biosynthesis of ZnO-NPs using parsley extract

Fifty grams of dry leaves and roots of parsley were washed by deionized water then were submerged in 50-ml water and heated at 70–80 °C for 20 min in a water bath. The extract was filtered using Whatman filter paper No. 1 and the volume was adjusted to 100 ml by washing the vegetal residue with ultrapure water (Stan et al. 2015). For the green biosynthesis ZnO-NPs, 50 ml of parsley aqueous extract was heated at 85–90 °C and 5 g of zinc acetate dehydrates was added then the mixture was heated at 90 °C under continual stirring for 3 h in light. The supernatant was filtrated and kept for 72 h at room temperature then heated for 24 h at 90 °C to obtain ZnO-NPs (Hajiashrafi and Motakef-Kazemi 2018). The ZnO-NPs were collected by centrifugation (10000 rpm for 10 min) and washed with distilled water and followed by ethanol to remove the remaining Zn^{2+} during the reaction mixture then sonicated several times before subjected to centrifugation. The collected ZnO NPs were then dried at 100 °C.

Thyme essential oil extraction

The thyme plant materials (100.0 g) were placed in 1 l of water in a round-bottomed flask connected with Clevenger-type

apparatus, and the hydro-distillation was performed for 4 h by boiling of water (Fadil et al. 2015). The resulted essential oil was dehydrated using sodium sulfate anhydrous and stored at 4 °C until used.

GC-MS analysis of TEO

GC-MS analysis was conducted using Hewlett-Packard model 5890 with a flame ionization detector (FID) and DB-5 fused silica capillary column (60 m × 0.32 mm). The temperature of the oven was maintained initially at 50 °C for 5 min and then programmed from 50 to 250 °C at a rate of 4 °C/min. The carrier gas was helium at a flow rate of 1.1 ml/min. The temperatures of the detector and injector were 250 and 220 °C, respectively, and the retention indices (Kovats index) of the separated volatile components were calculated using hydrocarbons as references (C7-C20, Aldrich Co.) as shown by Adams (2007).

Preparation of emulation solution of encapsulated thyme oil

MD, GA, and WPI were dissolved in distilled water with stirring. Solutions were kept overnight at room temperature before emulsification. Tween 80 (80 mg) was added to the polymer mixture as an emulsifier. Then, essential oils were progressively added to the polymer solution with homogenization at 20000 rpm for 10 min to form an emulsion. The polymer concentration was 20%, and the amount of essential oil used was 10% of the mass of the polymer concentration (Tomazelli Júnior et al. 2018). The emulsion solution was encapsulated by spray drying using a spray drier (B-290, *Buchi*) equipped with a pressure air atomizing nozzle at 2.5 bar, inlet temperature of 160 ± 5°C, and outlet air temperature of 85 ± 5°C. The dried encapsulated oil powder was collected and stored in the refrigerator at 4°C until used.

Characterization of ZnO-NPs and ETO

Transmission electron micrographs (TEMs) were recorded on JEOL JAX-840A and JEOL JEM-1230 electron micro-analyzers, respectively. The ZnO-NP samples were scattered in ethanol and then treated ultrasonically to disperse the individual particle over the gold grids (Mahamuni et al. 2019). However, for encapsulated thyme oil (ETO), the droplets were placed onto a carbon-coated copper grid to form a thin liquid film and were negatively stained by one drop of uranyl acetate. The excess of staining was removed using filter paper then the film was air-dried before the observation (Pecarski et al. 2014). The Orius 1000 CCD camera was used for image acquisition (GATAN, Warrendale, PA, USA). For measuring zeta potential, the sample of ZnO-NPs or ETO was sonicated for 30–60 min just before assessment. The average diameter was calculated using zpw 388 version 2.14 nicomp software. The size distribution and zeta potential of ZnO-NPs and ETO were measured using a particle size analyzer (Nano-ZS, Malvern Instruments Ltd., UK).

Experimental animals

Sexually mature male Sprague-Dawley rats (150–160 g; 3 months old) were purchased from AHC, National Research Center (NRC), Dokki, Cairo, Egypt. The animals were fed a standard laboratory diet (Meladco Feed Co., Aubor City, Cairo, Egypt) and housed in filter top polycarbonate cages in a room free from any source of chemical contamination, artificially illuminated (12 h dark/light cycle), and thermally controlled (25 ± 1 °C) at the Animal House Lab, NRC. All animals were received humane care in compliance with the guidelines of the Animal Care and Use Committee of NRC, Egypt, and the National Institute of Health (NIH publication 86-23 revised 1985).

Experimental design

Six groups of animals (10 rats/group) were preserved on their specific diet and treated orally for 3 weeks as follows: group 1, control animals received distilled water; group 2, rats received an aqueous solution of ZnO-NPs (25 mg/kg body weight); groups 3 and 4, rats received low (50 mg/kg body weight) or high (100 mg/kg body weight) dose of an aqueous solution of ETO; and groups 5 and 6, rats treated with a low or high dose of ETO (ETO(LD) and ETO(HD)) plus ZnO-NPs. The duration of the study and the selected doses of ZnO-NPs and ETO were derived from those reported in the previous studies (Khorsandi et al. 2016; Rojas-Armas et al. 2019). At the end of the experimental period (i.e., day 21), all animals were weighed after being fasted for 12 h, then blood samples were collected via the retro-orbital venous plexus under isoflurane anesthesia in non-ethylenediaminetetraacetic acid (EDTA)–containing vacutainer tubes. Sera were separated using cooling centrifugation and stored at −20 °C until analysis for the determination of different biochemical analyses, lipid profile, and serum cytokines according to the kit's instructions. After the collection of blood samples, animals were euthanized and samples of the spleen, femur bone marrow, livers, and kidneys of each animal were dissected. A sample of liver and kidney from each animal was weighed and homogenized in phosphate buffer (pH 7.4) using an ultrasound homogenizer (Sonics & Materials, INC. 53 Church Hill Rd. Newtown, CT, USA) as described by Lin et al. (1998) and the supernatants were used for the determination of MAD, NO, CAT, SOD, and TAC according to the kit's instructions. Other samples of the liver and kidney from each animal were fixed in 10% neutral formalin- and paraffin-embedded. Sections (5-μm

thickness) were stained with hematoxylin and eosin (H&E) for the histological examination (Drury and Wallington 1980).

Cytogenetic analysis

Single-cell electrophoresis (comet) assay

Alkaline comet assay was performed on bone marrow cells and spleen as described previously (Diab et al. 2018). The slides were stained with ethidium bromide and visualized at ×400 magnification under an epifluorescent microscope equipped with a digital camera and green excitation filter (510–560 nm) and barrier filter (590 nm). One hundred cells were analyzed per animal using comet score software (TriTek Corp, version 1.5., Sumerduck, VA22742, VA). The percentage of DNA in the comet tail (tail intensity) is considered to be the most reliable parameter to quantify DNA damage. The percentage of DNA in the comet tail (% tail DNA), tail moment (TM), and Olive tail moment (OTM) is the preferred comet tail parameter to quantify DNA breakage. The values of TM and OTM are expressed in arbitrary units (A.U) and the cells with > 80% DNA in the tail region were classified as hedgehogs and excluded from software analysis (Kumaravel et al. 2009).

Micronucleus assay

The MN assay was carried out in bone marrow cells according to Diab et al. (2018). The bone marrow slides were stained with May-Grünwald and Giemsa staining to discriminate between polychromatic erythrocytes (PCEs) and normochromatic erythrocytes (NCEs). Two thousand PCEs were analyzed per animal under light microscopy at ×1000 magnification for counting the frequency of micronucleated PCEs (MNPCEs). Five hundred total erythrocytes (PCEs + NCEs) were examined per animal, and the ratio of PCE/total erythrocytes was calculated to determine erythroblast proliferation rate or erythroblast cytotoxicity

Morphological apoptosis assay

The dual-fluorescent acridine orange and ethidium bromide (AO/EB) assay was performed for the observation of morphological apoptosis including chromosome condensation on bone marrow cells as described previously (Diab et al. 2018). Briefly, the slides were stained with a dual-fluorescent mixture of AO (5 mg/ml) and EB (5 mg/ml) for 2–5 min. In this assay, AO enters viable and nonviable cells and emits green or red fluorescence when binding to DNA or RNA, respectively. EB enters nonviable cells and emits orange or red fluorescence when binding to DNA or RNA, respectively. Hence, normal and apoptotic nuclei emit bright orange fluorescence in non-viability cases. Five hundred cells were examined per animal under an epifluorescent microscope at ×400 magnification with a blue excitation filter (480 nm) and a yellow emission barrier filter (515–530 nm). The apoptotic index was calculated according to the following formula: [number of apoptotic cells /total cell count] × 100.

Statistical analysis

The data were analyzed using computerized software SPSS (Statistical Package of Social Science, version 20, Armonk, New York: IBM Corp). One-way analysis of variance (ANOVA) followed by Duncan's multiple comparisons test was used to determine the difference among the experimental groups. The level of statistical significance was set at $P < 0.05$.

Results

The GC-MS analysis of the ETO revealed the identification of 13 bioactive compounds (Table 1) belongs to 5 classes including phenols, terpene, sesquiterpene, oxides, and oxygenated terpene. The majority of these compounds were phenols (carvacrol and thymol) followed by terpene (α and β-phellandrene, linalool, myrcene, α,β-pinene, β-sabinene, and tricyclene). Sesquiterpene (Humuline), oxides (1,8-cineole), and oxygenated terpene (α-thyjone) were found in a lesser concentration.

The results showed that the addition of 50 ml of heated parsley extract to 5 g zinc acetate dehydrates and stirring for 3 h then the filtration of the supernatant after 72 h resulted in the synthesis of ZnO-NPs. The TEM image of ZnO-NPs revealed that the particles are nearly spherical (Fig. 1A) with an

Table 1 Chemical constitutes of ETO identified by GC-MS

Constituents*	mg/g	Class
Carvacrol	45.8	Phenols
Thymol	25.70	Phenols
β-Phellandrene	10.20	Terpene
Linalool	5.10	Terpene
Humuline	3.70	Sesquiterpene
α-Phellandrene	2.40	Terpene
Myrcene	2.12	Terpene
β-Pinene	1.51	Terpene
1,8-Cineole	1.56	Oxides
α-Pinene	1.41	Terpene
β-Sabinene	1.34	Terpene
α-Thyjone	1.35	Oxygenated terpene
Tricyclene	1.11	Terpene
Total	103.3	

*Constituents presented in the order of concentration

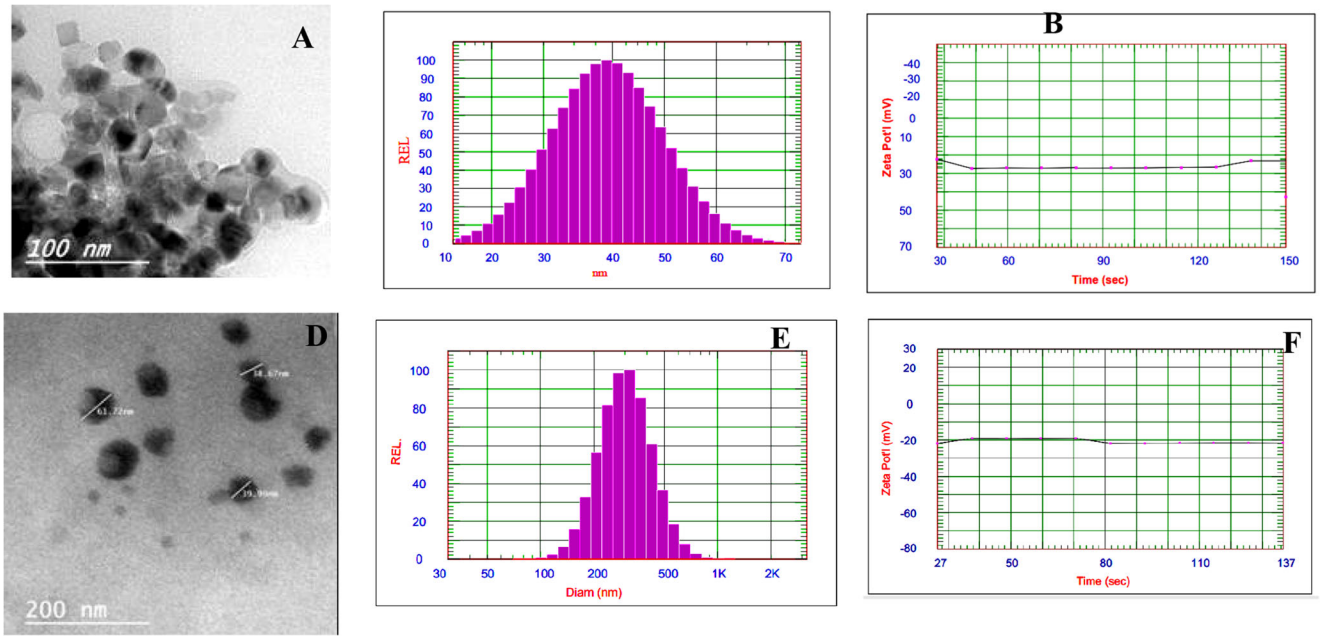

Fig. 1 TEM image of ZnO-NPs showing the nearly particle shape and size (A), DLS analysis showing the intens-wt Gaussian distribution of ZnO-NPs (B), frequency distribution of ZnO-NPs (C), ZetaSizer chromatogram showing the zeta potential of ZnO-NPs (D), TEM of ETO particle size and shape (E), DLS analysis showing the intens-wt Gaussian distribution of ETO (F), frequency distribution of ETO (G), and ZetaSizer chromatogram showing the zeta potential of ETO (H)

average particle size of 38 nm (Fig. 1B) and zeta potential of + 28.58 mV (Fig. 1C). The TEM image of ETO showed a rounded shape (Fig. 1D) with an average diameter of 311.8 ± 27 nm (Fig. 1E) and zeta potential of −21.63 mV (Fig. 1F).

The in vivo results showed a significant decrease in body weight in the animals treated with ZnO-NPs compared to the control group (Fig. 2). Animals treated with ETO at the low or the high doses were comparable to the control group. However, the combined treatment with ETO plus ZnO-NPs induced a significant improvement in body weight in a dose-dependent and the high dose could normalize the body weight. The results also revealed that the administration of ZnO-NPs induced a significant increase in AST, ALT, uric acid, urea, and creatinine; however, TP and Alb showed a significant decrease (Table 2). Animals that received ETO at the low or high dose were approximately similar to the untreated control group. The combined treatment with ETO plus ZnO-NPs improved significantly all the tested parameters and ETO at the high dose succeeded to normalize most of these parameters.

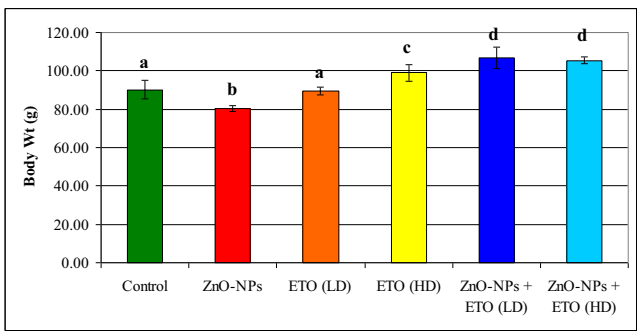

Fig. 2 Effect of encapsulated thyme oil (ETO) on body weight of rats treated with ZnO-NPs

The effect of ZnO-NP treatment alone or plus ETO on serum lipid profile (Table 3) indicated that ZnO-NP administration induced a significant increase in cholesterol, triglycerides, and LDL accompanied by a significant decrease in HDL. Animals who received ETO alone showed a significant decrease in cholesterol, triglycerides, and increased HDL but did not significantly affect LDL. Co-administration of ZnO-NPs and ETO induced a significant improvement in lipid profile parameters toward the control levels in a dose-dependent and most of these parameters were similar to the untreated control animals. The antioxidant parameters (TAC, CAT, and SOD) in the liver and kidney showed a significant decrease in the rats that received ZnO-NPs compared to the control rats (Table 4). These antioxidant parameters showed an insignificant increase in the groups treated with ETO in a dose-dependent. However, the combined treatment with ETO plus ZnO-NPs could improve these antioxidant parameters and the high dose was more efficacious than the low dose.

The effect of different treatments on oxidative markers MDA as the main product of lipid peroxidation and NO (Table 5) revealed that ZnO-NP administration significantly increased both parameters in the liver and kidney. No significant effect was observed in NO in both organs in animals that received ETO alone at the two doses. However, ETO decreased MDA in both organs in a dose-dependent manner. The combined treatment with ETO plus ZnO-NPs induced a

Table 2 Effect of ETO at low or high dose on serum biochemical parameters in rats treated with ZnO-NPs

Parameter Groups	ALT (U/L)	AST (U/L)	Alb (g/dl)	TP (g/dl)	Creatinine (mg/dl)	Uric acid (mg/dl)	Urea (mg/dl)
Control	53.60 ± 1.17[a]	134.80 ± 1.39[a]	6.56 ± 0.17[a]	6.20 ± 0.16[a]	0.54 ± 0.02[a]	5.70 ± 0.70[a]	35.0 ± 0.71[a]
ZnO-NPs	71.80 ± 0.97[b]	173.60 ± 4.30[b]	5.26 ± 0.33[b]	5.65 ± 0.13[b]	0.98 ± 0.02[b]	6.80 ± 0.16[b]	53.6 ± 1.44[b]
ETO(LD)	51.00 ± 2.43[a]	134.40 ± 0.81[a]	7.36 ± 0.14[c]	6.20 ± 0.13[a]	0.60 ± 0.04[c]	5.94 ± 0.12[a]	33.6 ± 1.83[a]
ETO(HD)	51.00 ± 1.34[a]	134.60 ± 1.44[a]	7.36 ± 0.14[c]	6.20 ± 0.15[a]	0.60 ± 0.03[c]	6.26 ± 0.31[c]	34.2 ± 1.24[a]
ZnO-NPs + ETO(LD)	58.58 ± 3.12[c]	139.60 ± 1.63[c]	7.30 ± 0.13[c]	5.76 ± 0.28[a]	0.62 ± 0.04[c]	5.98 ± 0.14[a]	46.2 ± 0.86[c]
ZnO-NPs + ETO(HD)	46.60 ± 2.16[d]	133.60 ± 2.38[a]	6.62 ± 0.08[a]	5.26 ± 0.33[c]	0.56 ± 0.05[a]	5.80 ± 0.10[a]	36.8 ± 1.16[a]

Within each column, means superscripts with different letters are significantly different ($P < 0.05$)

significant improvement in hepatic and renal MDA levels in a dose-dependent manner. In addition, ZnO-NP administration increased AFP, TNF-α, and CEA (Table 6); however, animals that received ETO at the two doses did not show any significant changes in AFP and TNF-α but the high dose decreased CEA significantly. Treatment with ZnO-NPs plus ETO(LD) or ETO(HD) could normalize AFP and TNF-α and decreased CEA compared to the control group (Table 6).

Comet assay

The data presented in Table 7 and Fig. 3 showed the effect of ZnO-NPs and ETO on the level of DNA breakages in bone marrow cells and spleen using the comet assay. In this assay, intact cells reflect high-molecular-weight genomic DNA and appear approximately rounded (comet head) or with a very short tail. The broken DNA migrates toward the anode leaving different patterns of the comet-like electrophoretic appearances. Administration of ZnO-NPs increased the percentage of tail DNA in bone marrow (9.41% vs 5.41% for the control) and spleen (16.39% vs 5.48% for the control). Consequently, tail moment (TM) and Olive tail moment (OTM) values were remarkably increased after treatment with ZnO-NPs in bone marrow (0.68 and 1.73 A.U, respectively) and spleen (1.54 and 3.25 A.U respectively) compared to their control values. Noteworthy, the incidence of hedgehog comet was observed in the ZnO-NP-treated group in bone marrow and spleen. By contrast, ETO at the tested doses did not induce any significant increase in all comet tail parameters in bone marrow and spleen compared to their control values. Interestingly, administration of ZnO-NPs plus ETO(LD) or ETO(HD) significantly decreased the percentage of tail DNA in bone marrow (8.10 and 7.66%, respectively) and spleen (12.66 and 11.79 %, respectively) compared to ZnO-NP alone–treated group. However, no significant differences were observed between the low- or high-dose groups in all comet tail parameters in the bone marrow and the spleen except tail moment in the spleen.

Micronucleus assay

As shown in Table 8, the administration of ZnO-NPs caused a 6-fold increase in MNPCE percentage (1.09% vs 0.18% for

Table 3 Effects of ETO on lipid profile in rats treated with ZnO-NPs

Parameter Groups	Cholesterol (mg/dl)	Tri G (mg/dl)	HDL (mg/dl)	LDL (mg/dl)
Control	61.40 ±1.96[a]	131.60 ± 2.06[a]	48.00 ± 1.34[a]	6.16 ± 0.35[a]
ZnO-NPs	80.20 ± 3.71[b]	145.40 ± 0.51[b]	31.00 ± 1.38[b]	7.12 ± 0.79[b]
ETO(LD)	51.00 ± 1.14[c]	133.80 ± 1.46[a]	50.40 ± 2.25[c]	6.08 ± 0.58[a]
ETO(HD)	48.20 ± 2.60[c]	119.20 ± 3.22[c]	52.40 ± 1.44[ac]	6.03± 0.71[a]
ZnO-NPs + ETO(LD)	66.40 ± 1.69[d]	138.00 ± 1.38[d]	45.40 ± 1.12[d]	6.68 ± 0.43[c]
ZnO-NPs + ETO(HD)	64.60 ± 1.72[d]	134.40 ± 4.76[a]	47.20 ± 1.53[a]	6.48 ± 0.24[c]

Within each column, means superscripts with different letters are significantly different ($P < 0.05$)

Table 4 Effects of ETO on antioxidant parameters in rats treated with ZnO-NPs

Parameter Groups	TAC (μM/g tissue)		CAT (mU/g tissue)		SOD (U/g tissue)	
	Liver	Kidney	Liver	Kidney	Liver	Kidney
Control	27.32 ± 1.34^{a}	26.89 ± 1.52^{a}	10.23 ± 1.03^{a}	9.32 ± 0.15^{a}	35.42 ± 1.37^{a}	31.21 ± 1.56^{a}
ZnO-NPs	20.28 ± 1.58^{b}	13.06 ± 0.27^{b}	6.25 ± 0.43^{b}	6.33 ± 0.53^{b}	18.22 ± 1.42^{b}	16.37 ± 1.41^{b}
ETO(LD)	27.65 ± 0.70^{a}	24.55 ± 1.73^{c}	10.66 ± 0.42^{a}	9.44 ± 0.43^{a}	36.14 ± 1.44^{a}	33.35 ± 0.73^{a}
ETO(HD)	28.32 ± 0.67^{a}	25.9 ± 2.45^{a}	11.32 ± 0.54^{c}	9.78 ± 0.44^{a}	38.72 ± 1.23^{c}	33.23 ± 1.31^{a}
ZnO-NPs + ETO(LD)	23.77 ± 0.35^{c}	17.83 ± 0.59^{d}	7.26 ± 0.75^{d}	8.23 ± 0.63^{c}	25.33 ± 1.47^{d}	23.42 ± 1.37^{c}
ZnO-NPs + ETO(HD)	25.36 ± 0.67^{d}	25.87 ± 1.59^{a}	8.12 ± 0.32^{e}	9.21 ± 0.52^{a}	33.43 ± 1.32^{a}	26.77 ± 1.32^{d}

Within each column, means superscripts with different letters are significantly different ($P < 0.05$)

the control, $p<0.05$) in bone marrow cells. However, no significant differences were observed in the percentage of MNPCE after treatment with ETO at the two doses (0.20 % and 0.24 %, respectively) compared to the control group. Co-treatment with ZnO-NPs and ETO at both doses significantly reduced the percentage of MNPCE (0.33% and 0.46%, respectively, $p< 0.05$) compared to the ZnO-NP alone–treated group. As depicted in Fig. 4, the observed micronuclei were varied in size (small or large) and shape (dot or round). Surprisingly, no significant difference ($p<0.05$) in the ratio of PCE/total erythrocytes was observed in all treated animals compared to the untreated control animals.

Morphological apoptosis assay

As depicted in Fig. 5, intact cells were surrounded by regular cell membranes without chromatin condensation. The early apoptotic cells were still bounded with irregular cell membranes containing patches of condensed chromatin distributed in the nuclear periphery. The late apoptotic cells appeared as a grape-like cluster containing protrusion of chromatin distributed in a few spherical apoptotic bodies. As shown in Fig. 6, treatment with the two tested doses of ETO did not dramatically produce any increase in the apoptotic rate compared to the control group. However, ZnO-NP treatment resulted in a significant increase in the apoptotic rate (11.96% vs 6.44% for the control, $p<0.05$) due to the increasing number of the cells in the early apoptotic phase. Supplementation with ETO at the low or high dose significantly suppressed ZnO-NP-induced apoptotic rate from 11.96 to 8.88 and 7.60%, respectively.

The examination of liver sections revealed the control liver showed normal architecture with a classic hepatic lobule–containing central vein and radiating cords of hepatocytes with blood sinusoids in between, polyhedral hepatocytes with large, rounded vesicular nuclei. The blood sinusoids are present in between the cords of hepatocytes and are lined by flattened endothelial cells and Kupffer cells (Fig. 7A). The liver sections of animals that received ZnO-NPs showed hepatocytes vacuolar degeneration and pyknotic nuclei (Fig. 7B). The liver of rats treated with ETO(LD) showed normal hepatocytes around the central vein (Fig. 7C). Moreover, the liver of rats treated with ETO(HD) showed nearly normal hepatocytes around the normal central vein (Fig. 7D). The liver sections of the rats treated with ZnO-NPs plus ETO(LD) showed no remarkable changes in hepatocytes and their blood vessel

Table 5 Effects of ETO on MDA and NO in rats treated with ZnO-NPs

Parameter Groups	NO (μmol/g tissue)		MDA (nmol/g tissue)	
	Liver	Kidney	Liver	Kidney
Control	2.55 ± 0.09^{a}	2.17 ± 0.04^{a}	37.96 ± 3.31^{a}	89.06 ± 1.80^{a}
ZnO-NPs	5.43 ± 0.07^{b}	4.53 ± 0.24^{b}	81.74 ± 0.17^{b}	180.04 ± 2.61^{b}
ETO(LD)	2.57 ± 0.06^{a}	2.18 ± 0.08^{a}	35.78 ± 2.70^{a}	84.54 ± 5.51^{c}
ETO(HD)	2.54 ± 0.08^{a}	2.25 ± 0.21^{a}	33.2 ± 7.40^{c}	81.98 ± 3.95^{c}
ZnO-NPs + ETO(LD)	3.98 ± 0.03^{c}	2.88 ± 0.13^{ac}	44.7 ± 2.01^{d}	125.60 ± 4.98^{d}
ZnO-NPs + ETO(HD)	3.11 ± 0.11^{c}	2.32 ± 0.32^{ac}	33.67 ± 1.60^{c}	95.87 ± 7.63^{a}

Within each column, means superscripts with different letters are significantly different ($P < 0.05$)

Table 6 Effects of ETO on serum cytokines in rats treated with ZnO-NPs

Parameter Groups	AFP (ng/ml)	TNF-α (ng/ml)	CEA (ng/ml)
Control	0.03 ± 0.01^{a}	0.27 ± 0.01^{a}	2.57 ± 0.07^{a}
ZnO-NPs	0.07 ± 0.00^{b}	0.39 ± 0.04^{b}	2.76 ± 0.22^{b}
ETO(LD)	0.03 ± 0.01^{a}	0.25 ± 0.02^{c}	1.54 ± 0.15^{c}
ETO(HD)	0.03 ± 0.01^{a}	0.24 ± 0.02^{c}	1.48 ± 0.22^{c}
ZnO-NPs + ETO(LD)	0.23 ± 0.17^{c}	0.25 ± 0.02^{c}	1.77 ± 0.08^{d}
ZnO-NPs + ETO(HD)	0.04 ± 0.03^{d}	0.27 ± 0.01^{a}	1.08 ± 0.06^{e}

Within each column, means superscripts with different letters are significantly different ($P < 0.05$)

architecture (Fig. 7E). Furthermore, the liver of rats that received ZnO-NPs plus ETO(HD) showed marked improvement in the hepatocytes' histological architecture and a marked decrease in inflammatory cells (Fig. 7F).

The examination of kidney sections of the control rats showed normal histology of glomeruli and renal proximal and distal convoluted tubules (Fig. 8A). However, the kidney of the rats that received ZnO-NPs showed swelling of the tubular lining epithelium with variable degrees of granular and single-cell necrosis and nuclear pyknosis among the tubular epithelium, diminished and distorted glomeruli, and atrophy of the glomerular tufts with mesangial necrosis (Fig. 8B). The kidney of rats treated with ETO(LD) or ETO(HD) showed nearly normal renal tubules and glomeruli (Fig. 8C, D). The kidney sections of the rats treated with ZnO-NPs plus ETO(LD) showed marked improvement in renal tubules and glomeruli cellularity (Fig. 8E). The kidney sections of the rats treated with ZnO-NPs plus ETO(HD) showed foci of epithelial cell necrosis (Fig. 8F).

Discussion

The results of the GC-MS analysis of the thyme essential oil revealed the occurrence of 13 compounds belonging to phenolic and terpene. Previous reports indicated that the majority of compounds in thyme oil are carvacrol and thymol (Rota et al. 2007). In this concern, Ahmad et al. (2014) isolated 22 compounds and the majority was thymol and p-cymene; however, Borugă et al. (2014) isolated 15 compounds and the majority was p-cymene, γ-terpinene, and thymol. Razzaghi-Abyaneh et al. (2009) also isolated 7 compounds from thyme essential oil and these authors suggested that the variation in the chemical composition may be due to the variety of the plane and the geographical regions

Recently, there is a growing interest in the synthesizing of ZnO-NPs through biological methods (El-Seedi et al. 2019). The development of such a new approach is mainly linked to the safety, eco-friendly, and cost-effectiveness besides the reduction of high energy or the decrease of the toxic chemicals used in the biological syntheses (Khalid et al. 2017; Krol et al. 2017). In the current study, the addition of zinc acetate to the parsley extract then submitted to thermal treatment led to the biosynthesis of ZnO-NPs nearly spherical in shape, the particle size of 38 nm, and zeta potential of + 28.58 mV. Similar particle size, shape, and zeta potential were reported by Hajiashrafi and Motakef-Kazemi (2018) who synthesized ZnO-NPs using parsley extract at 90 °C or other plant extracts (Kumar et al. 2014). These authors and others reported that the particle size and morphology of the produced ZnO-NPs were affected by pH variations, the concentration of zinc, the temperature, and the reaction time (Bala et al. 2015). Additionally, MD, GA, and WPI were successfully used in the encapsulation of the oil in a ratio of 2:1 (polymer:oil) and the encapsulated oil showed similar characteristics to those reported using different polymers such as chitosan to protect the oil from oxidation and to improve its characteristics (Mohammed et al. 2020)

In the current study, we defined various effects of ZnO-NPs in rats. The majority of these effects were the significant changes in body weight and the indices of blood chemistry, the alteration in antioxidant enzyme activity, the cytokines, cytogenetic, and the histological structure of the liver and kidney. Although the FDA recognized that micron-sized zinc

Table 7 Effect of ETO on the comet tail parameters in bone marrow and spleen of rats treated with ZnO-NPs (instead of Fig. 4)

Experimental groups	Bone marrow			Spleen		
	% tail DNA	TM	OTM	% tail DNA	TM	OTM
Control	5.41 ± 0.13^{a}	0.30 ± 0.02^{a}	1.06 ± 0.02^{a}	5.48 ± 0.37^{a}	0.31 ± 0.03^{a}	1.04 ± 0.07^{a}
ZnO-NPs	9.41 ± 0.41^{c}	0.68 ± 0.06^{d}	1.73 ± 0.11^{c}	16.39 ± 0.34^{c}	1.54 ± 0.08^{c}	3.25 ± 0.09^{c}
ETO(LD)	5.88 ± 0.24^{a}	0.29 ± 0.01^{a}	1.03 ± 0.05^{a}	5.82 ± 0.10^{a}	0.35 ± 0.02^{a}	1.18 ± 0.03^{a}
ETO(HD)	6.06 ± 0.19^{a}	0.40 ± 0.04^{ab}	1.21 ± 0.08^{a}	6.31 ± 0.17^{a}	0.42 ± 0.02^{a}	1.23 ± 0.02^{a}
ZnO-NPs + ETO(LD)	8.10 ± 0.43^{b}	0.58 ± 0.05^{cd}	1.46 ± 0.08^{b}	12.67 ± 0.44^{b}	1.49 ± 0.12^{c}	2.98 ± 0.13^{b}
ZnO-NPs + ETO(HD)	7.66 ± 0.27^{b}	0.50 ± 0.04^{bc}	1.42 ± 0.04^{b}	11.79 ± 0.47^{b}	1.26 ± 0.12^{b}	2.78 ± 0.13^{b}

Data expressed as mean % ± S.E. Within each column, the values % with different superscript letters are statistically different ($P<0.05$)

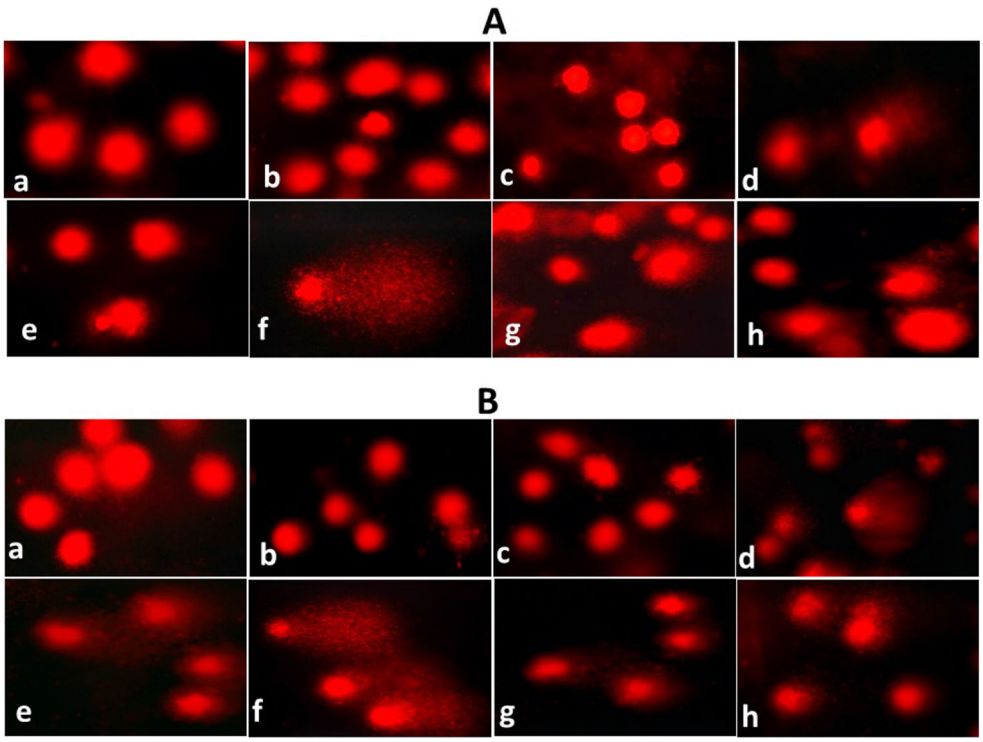

Fig. 3 Fluorescent images represented DNA damage in rat bone marrow (A) and spleen (B) showing: (a) control group; (b) ETO(LD); (c) ETO(HD); (d, e, f) ZnO-NPs; (g) ZnO-NPs + ETO(LD); ZnO-NPs + ETO(LH) (original magnification ×400)

oxide (ZnO) is a safe material, the safety of ZnO-NPs for animal consumption did not determine yet. The current results showed that administration of ZnO-NPs increased AST, ALT, uric acid, urea, and creatinine and decreased TP and Alb. The AST and ALT are the potent biochemical indices for the detection of the damage of liver tissue (Srivastav et al. 2016; Tang et al. 2016). The increase in these enzymes reported herein suggested that ZnO-NPs altered the permeability of the hepatocellular membrane (Yousef et al. 2019). In this concern, Kuznetsov et al. (2020) reported that the covalent binding of a drug to the intracellular proteins induces a reduction in adenosine triphosphate (ATP) level leading to the actin disruption and the rupture of the cell membrane. Moreover, it was reported that in the oral administration, ZnO may be dissolved in the stomach because of the acidic condition resulting in the formation of Zn^{+2} leading to cause significant toxicity (Srivastav et al. 2016). Similar observations were reported by Wang et al. (2006) in mice treated with nano- and micro-scale zinc powder. Moreover, urea, uric acid, and creatinine are considered the best indicators for renal function and they increase dramatically during kidney dysfunction. Our results indicated that these kidney indices increased in animals treated with ZnO-NPs suggesting that these particles affect the filtration rate of the glomerular and the ability of the kidney to induce blood filtration (Yousef et al. 2019). Moreover, the decreased level of TP and Alb in the group treated with ZnO-

Table 8 Effect of ETO on the incidence of micronucleated polychromatic erythrocytes (MNPCEs) and erythroblast cytotoxicity in rats treated with ZnO-NPs

Experimental groups	No. and % of MNPCE/2000 PCEs		PCE/(NCE+PCE)
	No.	Mean % ± SE	Mean % ± SE
Control	13	0.13 ± 0.03^{a}	0.48 ± 0.02^{a}
ZnO-NPs	109	1.09 ± 0.10^{d}	0.47 ± 0.02^{a}
ETO(LD)	20	0.20 ± 0.04^{ab}	0.44 ± 0.01^{a}
ETO(HD)	23	0.23 ± 0.03^{ab}	0.46 ± 0.03^{a}
ZnO-NPs + ETO(LD)	33	0.46 ± 0.04^{c}	0.45 ± 0.03^{a}
ZnO-NPs + ETO(HD)	46	0.33 ± 0.04^{bc}	0.49 ± 0.02^{a}

Total 10000 PCEs were analyzed per group (2000 PCE were analyzed per rat; 5 rats/group). The means % with different superscript letters are statistically significant different ($P<0.05$) using ANOVA followed by Duncan's multiple comparisons test

Within each column, means superscripts with different letters are significantly different ($P < 0.05$)

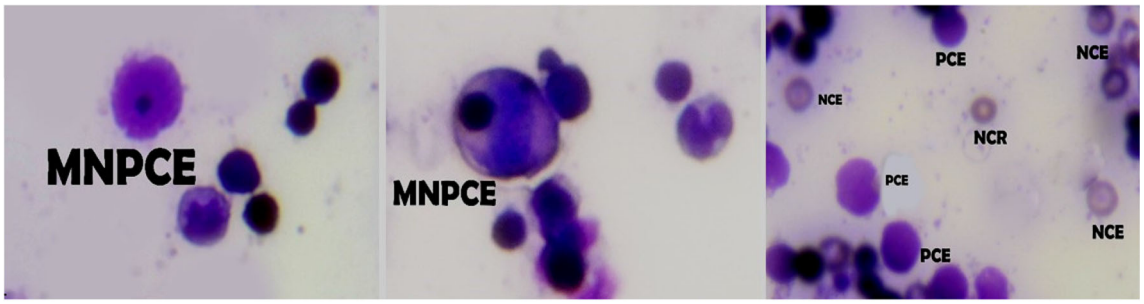

Fig. 4 Light microscope photomicrographs from rat bone marrow cells showing polychromatic erythrocyte (PCE); normochromatic erythrocyte (NCE); micronucleated polychromatic erythrocyte (MNPCE) (original magnification ×1000)

NPs suggested liver necrosis and/or kidney dysfunction (Abdel-Wahhab et al. 2007). Additionally, the decreased level of albumin may also be explained by its consumption for the defense against the oxidative stress of ZnO-NPs (Diab et al. 2015). Animals that received ZnO-NPs alone showed a significant increase in cholesterol, triglycerides, LDL, and a significant decrease in HDL suggesting a status of dyslipidemia. Dyslipidemia is considered a high-risk factor for coronary heart diseases (Allouche et al. 2011). Consequently, the current results indicated that ZnO-NPs are probably responsible for the disturbances in the lipid profile and the atherosclerosis risk (Moatamed et al. 2019).

The reduction in TAC, SOD, and CAT in hepatic and kidney of animals received ZnO-NPs and the elevation of MDA and NO indicated a status of oxidative stress and lipid peroxidation in the liver and kidney generated by the exposure to ZnO-NPs. According to Saliani et al. (2016), MDA is the main degradation product of the lipid peroxidation, whereas NO is an important free radical which induces severe damage to cells when produced excessively in the tissues or serum (Dillioglugil et al. 2012). A previous study reported oxidative stress–mediated cytotoxicity and DNA damage induced by ZnO-NPs in human HepG2 cells (Sharma et al. 2011). Moreover, Sha et al. (2014) showed that the generation of oxidative stress is the main mechanism of ZnO-NP toxicity. The current results are in accordance with the previous studies of Moatamed et al. (2019). Taken together, the decreased levels of antioxidants and the increased levels of MDA and NO confirmed that ZnO-NPs enhance the generation of ROS which include superoxide anions, hydrogen peroxide, and hydroxyl radicals, which thus cause oxidative damage to the cells and organs (Sharma et al. 2012; Tang et al. 2016). The current results also showed that ZnO-NP administration increased the serum TNF-α, AFP, and CEA suggesting the disturbance of the immune system. Tang et al. (2016) indicated that ZnO-NPs increased the white blood cell counts mainly granulocyte and neutrophil and decreased the lymphocyte count which reflects the inflammatory reaction and the immune dysfunction. Generally, the increased level of MDA, NO, TNF-α, AFP, and CEA and the decrease in TAC, SOD, and CAT suggested that the toxicity of ZnO-NPs is mainly via the production of reactive oxygen species (ROS) and inflammation (Ifeanyichukwu et al. 2020; Tian et al. 2015).

The in vivo genotoxicity studies of ZnO-NPs are limited, are restricted to mice, and remain controversial. To explore the genotoxicity of ZnO-NPs, the combined comet DNA and micronucleus assays are recognized by international organizations (Kasamoto et al. 2017). Comet assay is generally measured DNA strand breaks, incomplete excision repair, and cross-linking sites in individual cells (Kang et al. 2013). However, the micronucleus test provides information about the structural or numerical abnormalities induced by clastogenic or aneugenic agents, respectively (Smart et al. 2019). The large- and small-sized micronuclei are represented as a whole chromosome or acentric fragment, respectively,

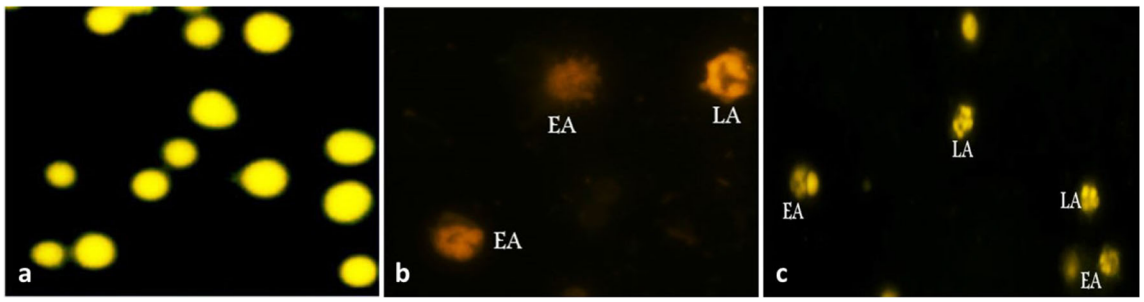

Fig. 5 Morphological changes in rat bone marrow cells stained with mixture of AO/EB showing (a) normal cells; (b, c) different stage of apoptosis including early apoptosis (EA) and late apoptosis (LA) (original magnification ×400). Early apoptosis (EA) and late apoptosis (LA)

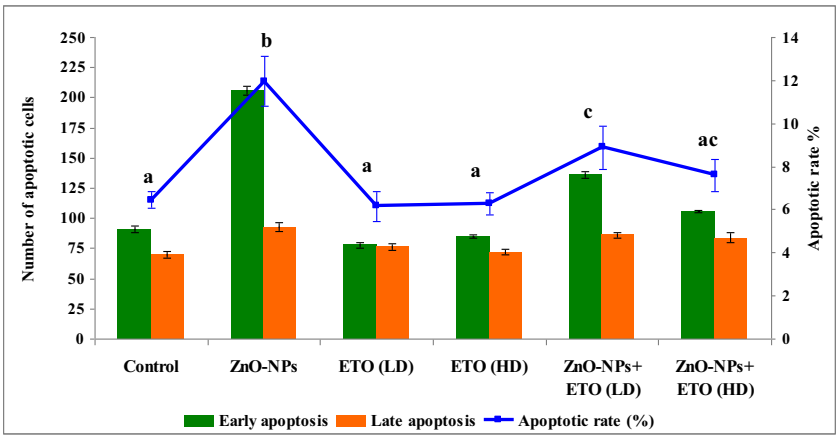

Fig. 6 Effect of ETO on the induction of morphological apoptotic events in bone marrow cells of rats treated with ZnO-NPs. Within each series, the values with different superscript letters are statistically different ($P<0.05$)

that dropped throughout the anaphase stage of the erythrocyte nucleus, during the degeneration process (Moras et al. 2017).

In the study, ZnO-NPs were positively genotoxicity in bone marrow cells, and spleen using the micronucleus test

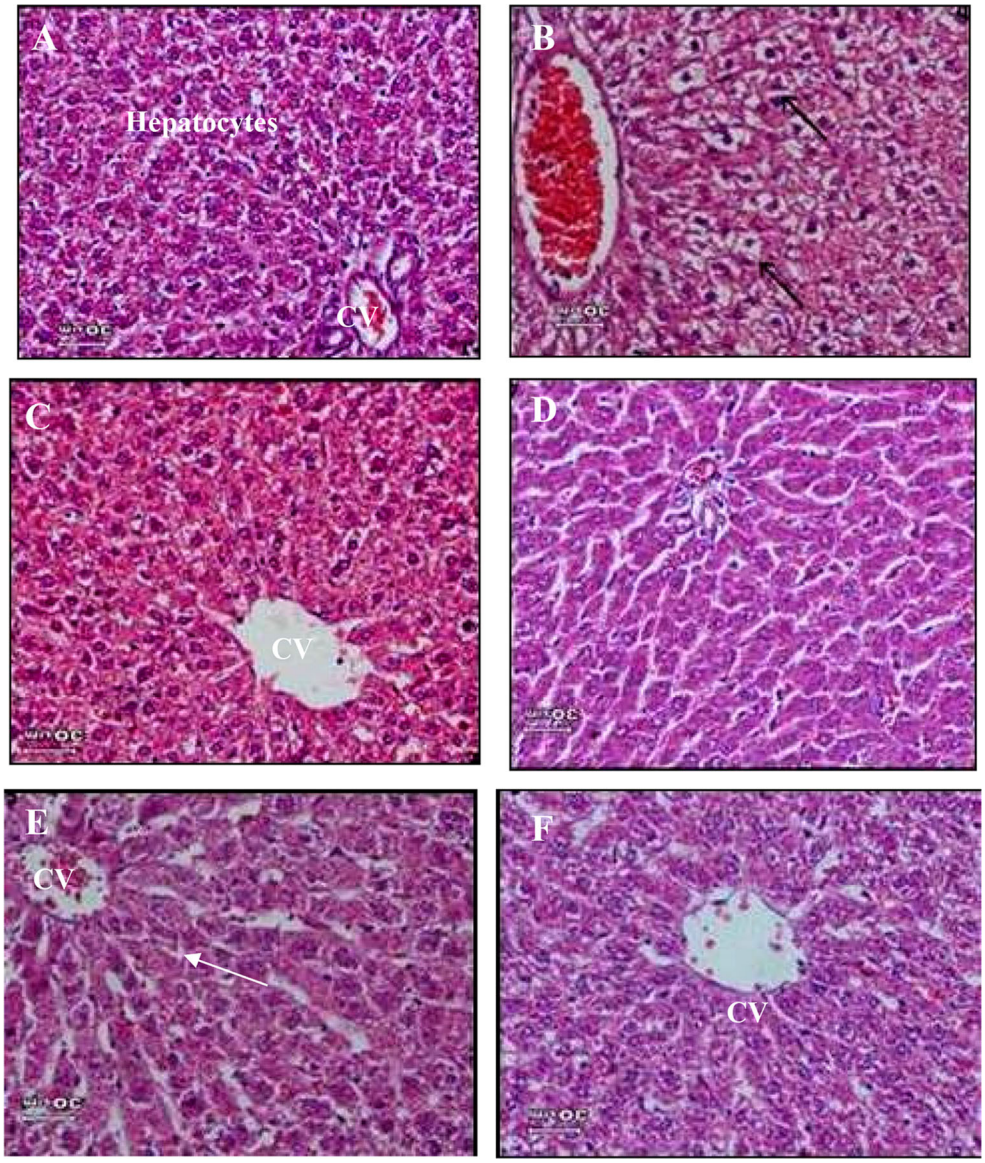

Fig. 7 Photomicrographs of the liver sections of (A) control rats showing normal central veins and hepatocytes; (B) rats treated with ZnO-NPs revealing hepatocyte vacuolar degeneration and pyknotic nuclei (arrows); (C, D) rats treated with low and high dose of ETO showing nearly hepatocytes and vesicle nuclei (arrows) and (E, F) rats treated with ZnO-NPs plus the low or the high dose ETO, respectively showing improvement in hepatic cells architectures (arrows) (H&E, ×400)

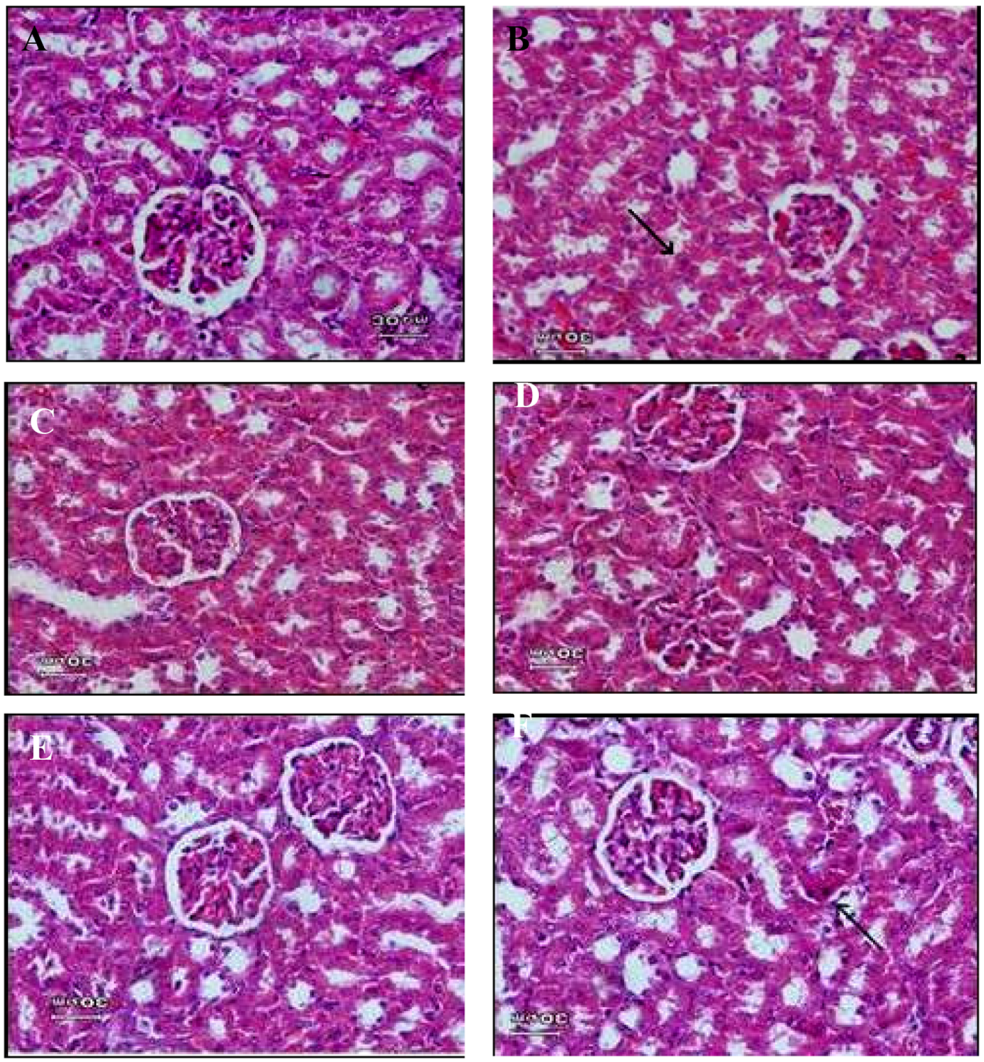

Fig. 8 Photomicrographs of the kidney sections of (A) control rats showing normal parenchyma, intact renal corpuscles with normal glomerular tufts; (B) rats treated with ZnO-NPs showing swelling of the tubular lining epithelium with variable degrees of granular and single cell necrosis and nuclear pyknosis among the tubular epithelium, diminished and distorted glomeruli, atrophy of the glomerular tufts with mesangeal necrosis (arrow); (C, D) rats treated with low or high dose of ETO showing nearly normal renal tubules and glomeruli and (E, F) rats treated with ZnO-NPs plus ETO showing foci of epithelial cells necrosis (arrow) (H&E, ×400)

and comet assay. These results are agreed with earlier in vitro and in vivo studies (Fadoju et al. 2019; Ghosh et al. 2016). Sharma et al. (2012) showed that the oral administration of ZnO-NPs induced DNA breakage in mouse liver, and Ghosh et al. (2016) found that single intraperitoneal exposure to ZnO-NPs induced genotoxicity in both the liver (comet assay) and bone marrow (chromosomal aberration and micronuclei). Likewise, Pati et al. (2016) exhibited that single oral inoculation with ZnO-NPs induced micronuclei in mice blood and bone marrow cells. However, another in vitro study reported that ZnO-NPs induced genotoxicity in human peripheral blood (Shalini et al. 2018), Chinese hamster lung fibroblasts (Reis Éde et al. 2015), Chinese hamster ovary (CHO-K1) cells, and human liver cancer HepG2 cells (Mohammad et al. 2019; Sharma et al. 2011).

It appears that the genotoxicity of ZnO-NPs depends on the following factors: (1) experimental conditions including the dosage, route of administration, treatment period, animal model, sensitivity of the cells, and genetic biomarkers; (2) physiochemical properties including shape, size, surface charged, and rate of agglomeration; (3) disparity in the biodistribution and accumulation of Zn^{+2} inside the tissues (Shalini et al. 2018; Singh 2019). Following the oral administration of Zn-NPs (20–120 nm in size), the liver, heart, pancreas, bone, and spleen are the target organs for its accumulation in mice (Wang et al. 2008). Surprisingly, ZnO-NPs had an insignificant impact on the ratio of PCE/total erythrocyte although it induced micronuclei formation in the bone marrow erythrocytes. This observation is agreed with Ghosh et al. (2016), who found that ZnO-NPs did not induce any significant reduction in the cytotoxicity of erythroblast in mouse bone marrow cells. Likewise, ZnO-NPs with a small particle size showed lower cytotoxicity and higher genotoxicity in human peripheral blood lymphocytes compared to ZnO-NPs with a large particle size (Shalini et al. 2018).

The dual-fluorescent AO/EB assay is used as an indicator of membrane integrity to assess apoptosis/cytotoxicity (Kasibhatla et al. 2006). In our study, ZnO-NPs elicited

cytotoxicity in whole nucleated bone marrow cells, as evidenced by the increase of apoptotic rate. These data implied that ZnO-NPs enter the body, are distributed throughout the body, and elicited cytotoxicity in different animal organs (Li et al. 2012). This outcome agreed with Zarria-Romero et al. (2017), who found that ZnO-NPs (1–10 mg/kg) reduced cell viability in bone marrow cells of mice using MTT assay during 30 h from intraperitoneal inoculation. Further, the cytotoxic potential of ZnO-NPs has been documented in mouse bone marrow mesenchymal stem cells (Syama et al. 2014), and human blood cells (Shalini et al. 2018) using MTT assay. Similarly, ZnO-NPs induced cytotoxic, genotoxic, and anticancer activities at low concentrations in human promyelocytic leukemia HL-60 (Soni et al. 2017), cervical (HeLa), and lung (NCI-H460) cancer cell lines (Esparza-Gonzalez et al. 2016). In this context, ZnO-NPs are selected as chemotherapeutic drugs due to their selective toxicity to preferentially kill cancer cells with minimal toxicity toward normal human cells (Gümüş et al. 2014). It appears that genotoxicity and cytotoxicity of ZnO-NPs with small particle sizes may be attributed to the rapid dissolution of Zn^{+2} in the aqueous solution (Mudunkotuwa et al. 2012). The release of Zn^{+2} can easily disrupt the cell membrane, induce ROS generation, impair the mitochondria, and induce genotoxicity and cell death (Sharma et al. 2012; Wang et al. 2014).

The histological examination of the hepatic and renal sections in rats that received ZnO-NPs showed severe histological changes typical to those reported in the previous studies (Moatamed et al. 2019; Shaban et al. 2019). These findings confirmed the biochemical results reported herein and supported the hypothesis that ZnO-NPs induced severe hepatonephrotoxicity mainly through the generation of oxidative damage and the immunodeficiency response.

The antioxidant and prophylactic activity of ETO is scarce and focused on its main chemical constituents (thymol and carvacrol), and hepatoprotective activity in rodents (El-Nekeety et al. 2011; Grespan et al. 2014). In recent years, more efforts were focused on the encapsulation of essential oils to reduce their high volatility, toxicity, and decomposition. In this sense, it is necessary to re-evaluate ETO to ensure its safety and prophylactic activity. Animals administrated ETO at the low or the high doses alone were comparable to the control, and the combined treatments with ZnO-NPs plus ETO showed potential protection against ZnO-NPs toxicity. Most of the tested parameters showed significant improvement toward the control values and the high dose was more effective. Similar observations were reported by Bouhtit et al. (2021), Ündeğer et al. (2009), and El-Nekeety et al. (2011) who suggested that carvacrol and thymol exhibited higher antioxidants in cell-free assay than Trolox. Moreover, thymol decreased ROS production and inhibited hepatotoxicity induced by CCl_4 (Rašković et al. 2015). The use of encapsulated thyme oil induced more protection since the encapsulation increased the antioxidant efficiency of the oil (Gonçalves et al. 2017).

Moreover, phenolic thymol and carvacrol were found to induce the high antioxidative effect of LDL and decrease plasma levels of triglycerides and cholesterol without adverse effects in kidneys or liver (Ebenyi et al. 2012). Additionally, they act on inflammatory by preventing the proinflammatory factor secretion via the decrease of lipopolysaccharide (LPS) (De Andrade et al. 2017). Moreover, carvacrol, the phenolic compounds in the EOs of thyme, induced apoptosis in metastatic breast cancer cell line MDA-MB-231 through the permeabilization of mitochondrial membrane, consequently the release of cytochrome C, induction of the caspases, and DNA fragmentation (Arunasree 2010). These compounds also are important free radical scavengers' natural products and possess antioxidant properties (Ebenyi et al. 2012). Besides, this oil may increase the level of other natural antioxidants in the body, such as GSH, SOD, and CAT, which protect the liver from PAR-induced hepatotoxicity (El-Banna et al. 2013). The hepatoprotective activities of ETO may be through the improvement of hepatocyte function by (i) the inhibition of cytochrome P450 activity, (ii) the acceleration of parenchyma cells regeneration, (iii) stabilizing the membrane of the hepatocytes, (iv) the enhancement of antioxidant activity, and (v) a combination of the all-aforementioned factors (Al-Fartosi et al. 2011).

The genotoxicity results indicated that ETO alone at the two tested doses had no response in rat bone marrow cells and spleen, indicating its safety. In agreement with this view, ETO is classified as moderately toxic and falls into category 4 (> 300–2,000 mg/kg body weight) with an LD_{50} cutoff value (1000 mg/kg) in rats (Rojas-Armas et al. 2019). Similarly, oral administration of carvacrol (81, 256, or 810 mg/kg) did not induce mutagenic activity in rat bone marrow cells using micronucleus and comet assay (Esparza-Gonzalez et al. 2016). Likewise, "in vitro" studies for carvacrol and thymol exhibited no mutagenic effect in Chinese hamster lung fibroblast (V79) cells (Ündeğer et al. 2009), human lymphocytes (Turkez and Aydin 2016), and mouse lymphoma cells (Maisanaba et al. 2015). Noteworthy, the loss of apoptotic activity of ETO in bone marrow cells is in harmony with the absence of its genotoxicity in our study. Indeed, apoptotic or cytotoxic activity is normally associated with extensive DNA fragmentation and is thus considered a secondary outcome of genotoxicity. Recently, thyme oil, carvacrol, and thymol did not exhibit cytotoxic activity (MTT assay) in mouse leukocytes obtained from its peritoneal cavity (Fachini-Queiroz et al. 2012).

Supplementation with ETO has successfully reversed the genotoxic and apoptotic activity induced by ZnO-NPs, in the spleen and bone marrow. These data implied that ETO interferes with ZnO-NPs and prevents attacking the DNA molecule. Similar studies exhibited the in vitro antimutagenic

activity of thyme oil and its chemical constituents (Khafaji 2018). For example, thymol and carvacrol had effectively geno-protective activity using comet assay in human cancer cells including leukemia K562 (Horvathova et al. 2007), liver HepG2, and colon Caco-2 (Horvathova et al. 2006). Due to a lack of apoptotic/cytotoxic activity of ETO in normal mammalian tissues, ETO is considered more suitable for food and pharmaceutical industries.

In the current study, WPI, MD, and GA were used in the encapsulation of the essential oil as a wall material; hence, we can propose another mechanism for ETO-induced protection. WPI is a well-known antioxidant and hepatoprotective agent (Gad et al. 2011) due to its ability to increase the level of tissue glutathione (Bayrama et al. 2009; Mohammed et al. 2020). It is rich in the amino acids cysteine, α-lactoglobulin, bovine serum albumin, and β-lactoglobulin (Rodzik et al. 2020). Cysteine is responsible for the regulation of GSH which responsible for the protection against the damage of cells (Kennedy et al. 2020). Additionally, MD is a polysaccharide well known to exhibit antioxidant activity (Wang et al. 2016) and can scavenge several ROS such as 2,2-diphenyl-1-picrylhydrazyl (DPPH), hydroxyl radical, H_2O_2, peroxyl radical, ABTS radical, superoxide radical, and alkyl radical and exhibit reducing power properties (Wang et al. 2017; Zhong et al. 2019). The antioxidant effects of polysaccharides can alleviate the risk of several diseases resulted from oxidative stress such as liver injury, neurodegenerative disease, breast cancer, obesity, colitis, and diabetes (Li et al. 2017) via three direct mechanisms including the scavenging of ROS, the regulation of the antioxidant system and oxidative stress–mediated signaling pathways. Hence, MD in the wall of ETO probably induces a synergistic protective activity and enhances the antioxidant activity of ETO in addition to its role in the scavenging of ROS generated by ZnO-NPs (Zhong et al. 2019). Additionally, the use of GA in the encapsulation process enhanced the protective activity of ETO. GA consists of branched chains of polysaccharides. Polysaccharides are being used to reduce experimental toxicity as it has strong antioxidant properties (Kong et al. 2014). Moreover, GA is well known to improve the antioxidant status of the human body and induce hepatoprotection by modulating the expression of several oxidative stress genes (Ahmed et al. 2015). A previous study also suggested that GA is rich in phenolics which are correlated to its antioxidant than its scavenging power (Edet et al. 2015; Mirghani et al. 2018; Sahu and Saxena 2013). GA was also reported to decrease superoxide production and MDA and increased TAC and GSH levels in rats (Ali et al. 2020). Furthermore, the antioxidant capacity of GA may be attributed to its content of different amino acids (Ali et al. 2020; Khalid et al. 2017); besides, it has anti-inflammatory and immune-modulatory actions in mice (Edet et al. 2015; Kamal et al. 2018) via attenuating C-reactive protein and TNFα and increasing the anti-inflammatory cytokine IL10 (Ali et al. 2013; Ushida et al. 2011).

Overall, the protective and antimutagenic activity of ETO is attributed to the antioxidant activity of the phenolic compounds in this oil and also the antioxidant activity of the materials used in the encapsulation process (i.e., WPI, GA, and MD). These compounds can inactivate the mutagens through multiple mechanisms, including (1) suppression of attacking off the mutagens into the DNA molecule; (2) scavenging of free radical produced by mutagens; (3) promoting DNA repair pathway; (4) stimulation of antioxidant defense system; (5) suppression lipid peroxidation (Bhalla et al. 2013; El-Nekeety et al. 2011; Grespan et al. 2014); and (6) the role of WP in the stimulation of a synergistic activity and the enhancement of GSH synthesis (Kerasioti et al. 2018).

Conclusion

The current study concluded that ZnO-NPs with a particle size of 38 nm can be synthesized by green chemistry using parsley extract. Administration of ZnO-NPs to rats induced severe toxicity and oxidative stress leading to biochemical changes including liver and kidney indices, the disturbances of lipid profile, oxidative damage, cytotoxicity, and histological changes in the liver and kidney. Encapsulation of thyme essential oil in whey protein enhanced the antioxidant activity of the oil and protect against the oxidative damage of ZnO-NPs. In this study, we achieved several goals including (1) the ability to produce ZnO-NPs with particle size of 38 nm using green chemistry, (2) evaluate the oxidative stress and cytotoxicity of ZnO-NPs in rats, and (3) evaluate the protective role of encapsulated thyme essential oil against oxidative stress of ZnO-NPs. These protective properties were due to the synergistic effects of the bioactive phenolic compounds in the oil as well as the protective role of WPI, MD, and GA used in the encapsulation. Consequently, ETO may be a suitable candidate for food and pharmaceutical applications.

Availability of data and materials Data are available on request to the authors

Author contribution This work was carried out in collaboration between all authors. Authors ME Hassan, RR Hassan, KA Diab, AA El-Nekeety, and NS Hassan carried out the experimental work, managed the literature searches, and shared in writing the first draft of the manuscript. Author MA Abdel-Wahhab wrote the protocol, managed the project, managed the analyses of the study, performed the statistical analysis, and wrote the final draft of the manuscript. All authors read and approved the final manuscript.

Funding This work was supported by the National Research Centre, Dokki, Cairo, Egypt project no. 12050305.

Declarations

Ethical approval All animals received humane care in agreement with the guidelines of the Animal Care and Use Committee of the National Research Center, Dokki, Cairo, Egypt, and the National Institute of Health (NIH publication 86-23 revised 1985) under the ethical approval no. 12050305 (Dec 2019).

Consent to participate Not applicable

Consent for publication Not applicable

Competing interests The authors declare no competing interests.

References

Abdel-Wahhab MA, Abdel-Galil MM, Hassan AM, Hassan NH, Nada SA, Saeed A, El-Sayed MM (2007) *Zizyphus spina-christi* extract protects against aflatoxin B_1-intitiated hepatic carcinogenicity. Afr J Trad CAM 4(3):248–256

Abdel-Wahhab MA, El-Nekeety AA, Hassan NS, Gibriel AA, Abdel-Wahhab KG (2018) Encapsulation of cinnamon essential oil in whey protein enhances the protective effect against single or comined sub-chronic toxicity of fumonisin B_1 and/or aflatoxin B_1 in rats. Environ Sci Pollut Res 25(29):29144–29161

Adams RP (2007) Identification of essential oil components by gas chromato-graphy/mass spectroscopy, vol 432. Allured Publishing Crop, Carol Stream, Illinois

Ahmad A, van Vuuren S, Viljoen A (2014) Unravelling the complex antimicrobial interactions of essential oils, the case of *Thymus vulgaris* (thyme). Molecules 19(3):2896–2910

Ahmed AA, Fedail JS, Musa HH, Kamboh AA, Sifaldin AZ, Musa TH (2015) Gum Arabic extracts protect against hepatic oxidative stress in alloxan induced diabetes in rats. Pathophysiol. 22:189–194

Al-Fartosi KG, Khuon OS, Al-Tae HI (2011) Protective role of camel's milk against paracetamol induced hepatotoxicity in male rats. Int J Res Pharmaceut Biomed Sci 2:1795–1799

Ali BH, Beegam I, Al-Lawati M, Waly MI, Al Za'abi M, Nemmar A (2013) Comparative efficacy of three brands of gum acacia on adenine-induced chronic renal failure in rats. Physiol Res 62(62): 47–56

Ali NE, Kaddam LA, Alkarib SY, Kaballo BG, Khalid SA, Higawee A, AbdElhabib A, AlaaAldeen A, Phillips AO, Saeed AM (2020) Gum Arabic (*Acacia Senegal*) augmented total antioxidant capacity and reduced C-reactive protein among haemodialysis patients in phase II trial. Int J Nephrol 2020:7214673. https://doi.org/10.1155/2020/7214673

Allouche L, Hamadouche M, Touabti A, Khennouf S (2011) Effect of long-term exposure to low or moderate lead concentrations on growth, lipid profile and liver function in albino rats. Adv Biol Res 5(6):339–347

Almansour MI, Alferah MA, Shraideh ZA, Jarrar BM (2017) Zinc oxide nanoparticles hepatotoxicity: histological and histochemical study. Environ Toxicol Pharmacol 51:124–130

Arunasree KM (2010) Anti-proliferative effects of carvacrol on a human metastatic breast cancer cell line, MDA-MB 231. Phytomed. 17(8-9):581–588

Bala N, Saha S, Chakraborty M, Maiti M, Das S, Basu R, Nandy P (2015) Green synthesis of zinc oxide nanoparticles using *Hibiscus subdariffa* leaf extract: effect of temperature on synthesis, anti-bacterial activity and anti-diabetic activity. RSC Adv 5:4993–5003

Bayrama T, Pekmez M, Arda N, Yalcın AS (2009) Antioxidant activity of whey protein fractions isolated by gel exclusion chromatography and protease treatment. Talanta 75:705–709

Bhalla Y, Gupta VK, Jaitak V (2013) Anticancer activity of essential oils: a review. J Sci Food Agric 93:3643–3653

Bin-Meferij MM, Hamida RS (2019) Biofabrication and antitumor activity of silver nanoparticles utilizing novel nostoc sp. Bahar M. Int J Nanomedicine 14:9019–9029

Borugă O, Jianu C, Mişcă C, Goleţ I, Gruia AT, Horhat FG (2014) *Thymus vulgaris* essential oil: chemical composition and antimicrobial activity. J Med Life 7(3):56–60

Bouhtit F, Najar M, Moussa Agha D, Melki R, Najimi M, Sadki K, Boukhatem N, Bron D, Meuleman N, Hamal A, Lagneaux L, Lewalle P, Merimi M (2021) New anti-leukemic effect of carvacrol and thymol combination through synergistic induction of different cell death pathways. Molecules 26(2):410. https://doi.org/10.3390/molecules26020410

De Andrade TU, Brasil GA, Endringer DC, Da Nobrega FR, De Sousa DP (2017) Cardiovascular activity of the chemical constituents of essential oils. Molecules 22(9):1539. https://doi.org/10.3390/molecules22091539

Diab AA, Zahralh MH, Al-dohim SI, Hassan NJ (2015) The impact of *Moringa oleifera* extract and vitamin E against zinc oxide nanoparticles induced hepatotoxicity in male albino rats. J Am Sci 11(5): 185–197

Diab KA, Fahmy MA, Hassan ZM, Hassan EM, Salama AB, Omara EA (2018) Genotoxicity of carbon tetrachloride and the protective role of essential oil of *Salvia officinalis L.* in mice using chromosomal aberration. micronuclei formation and comet assay. Environ Sci Pollut Res 25:1621–1636

Dillioglugil MO, Mekık H, Muezzinoglu B, Ozkan TA, Demir CG, Dillioglugil O (2012) Blood and tissue nitric oxide and malondialdehyde are prognostic indicators of localized prostate cancer. Int Urol Nephrol 44(6):1691–1696

Drury RAV, Wallington EA (1980) Carltons Histological Techniques, 5th edn. Oxford University Press, New York, p 206

Ebenyi LN, Ibiam UA, Aja PM (2012) Effects of *Allium sativum* extract on paracetamol–induced hepatotoxicity in albino rats. IRJBB 2:93–97

Edet E, Ofem J, Igile G, Ofem O, Zainab D, Akwaowo G (2015) Antioxidant capacity of different African seeds and vegetables and correlation with the contents of ascorbic acid, phenolics and flavonoids. J Med Plant Res 9:454–461

El-Banna H, Solimanand M, Al-Wabel N (2013) Hepatoprotective effects of Thymus and Salvia essential oils on paracetamol induced toxicity in rats. J Phys Pharm Adv 3:41–47

El-Nekeety AA, Mohamed SR, Hathout AS, Hassan NS, Aly SE, Abdel-Wahhab MA (2011) Antioxidant properties of *Thymus vulgaris* oil against aflatoxin-induce oxidative stress in male rats. Toxicon 57: 984–991

El-Seedi HR, El-Shabasy RM, Khalifa SAM, Saeed A, Shah A, Shah R, Iftikhar FJ, Abdel-Daim MM, Omri A, Hajrahand NH, Sabir JSM, Zou X, Halabi MF, Sarhann W, Gu W (2019) Metal nanoparticles fabricated by green chemistry using natural extracts: biosynthesis, mechanisms, and applications. RSC Adv 9:24539–24559

Esparza-Gonzalez SC, Sanchez-Valdes S, Ramirez-Barron SN, Loera-Arias MJ, Bernal J, Melendez-Ortiz HI, Betancourt-Galindo R (2016) Effects of different surface modifying agents on the cytotoxic and antimicrobial properties of ZnO nanoparticles. Toxicol in Vitro 37:134–141

Espitia PJP, Soares NFF, Coimbra JSR, Andrade NJ, Cruz RS, Medeiros EAA (2012) Zinc oxide nanoparticles: synthesis, antimicrobial activity and food packaging applications. Food Bioprocess Technol 5: 1447–1464

Fachini-Queiroz FC, Kummer R, Estevão-Silva CF, Carvalho MD, Cunha JM, Grespan R, Bersani-Amado CA, Cuman RK (2012)

Effects of thymol and carvacrol, constituents of *Thymus vulgaris L.* essential oil, on the inflammatory response. Evid Based Complement Alternat Med 2012:657026. https://doi.org/10.1155/2012/657026

Fadil M, Farah A, Ihssane B, Haloui T, Rachiq S (2015) Optimization of parameters influencing the hydrodistillation of Rosmarinus officinalis L. by response surface methodology. J Mat Environ Sci 6(8):2328–2336

Fadoju O, Ogunsuyi O, Akanni O, Alabi O, Alimba C, Adaramoye O, Cambier S, Eswara S, Gutleb AC, Bakare A (2019) Evaluation of cytogenotoxicity and oxidative stress parameters in male Swiss mice co-exposed to titanium dioxide and zinc oxide nanoparticles. Environ Toxicol Pharmacol 70:103204. https://doi.org/10.1016/j.etap.2019.103204

Gad AS, Khadrawy YA, El-Nekeety AA, Mohamed SR, Hassan NS, Abdel-Wahhab MA (2011) Antioxidant activity and hepatoprotective effects of whey protein and *spirulina* in rats. Nutr. 27(5):582–589

Ghosh M, Sinha S, Jothiramajayam M, Jana A, Nag A, Mukherjee A (2016) Cyto-genotoxicity and oxidative stress induced by zinc oxide nanoparticle in human lymphocyte cells *in vitro* and Swiss albino male mice *in vivo*. Food Chem Toxicol 97:286–296

Gonçalves ND, Pena FL, Sartoratto A, Derlamelina C, Duarte MCT, Antunes AEC, Prata AS (2017) Encapsulated thyme (*Thymus vulgaris*) essential oil used as a natural preservative in bakery product. Food Res Int 96:154–160

Grespan R, Aguiar RP, Giubilei FN, Fuso RR, Damião MJ, Silva EL, Mikcha JG, Hernandes L, Bersani Amado C, Cuman RK (2014) Hepatoprotective effect of pretreatment with *Thymus vulgaris* essential oil in experimental model of acetaminophen-induced injury. Evid Based Complement Alternat Med 2014:954136–954136

Gümüş D, Berber AA, Ada K, Aksoy H (2014) *In vitro* genotoxic effects of ZnO nanomaterials in human peripheral lymphocytes. Cytotechnol. 66:317–325

Hajiashrafi S, Motakef-Kazemi N (2018) Green synthesis of zinc oxide nanoparticles using parsley extract. Nanomed Res J 3(1):44–50

Hamida RS, Albasher G, Bin-Meferij MM (2020) Oxidative stress and apoptotic responses elicited by nostoc-synthesized silver nanoparticles against different cancer cell lines. Cancers 12(8):2099. https://doi.org/10.3390/cancers12082099

Hesabi Nameghi A, Edalatian O, Bakhshalinejad R (2019) Effects of a blend of thyme, peppermint and eucalyptus essential oils on growth performance, serum lipid and hepatic enzyme indices, immune response and ileal morphology and microflora in broilers. J Anim Physiol Anim Nutr (Berl) 103(5):1388–1398

Horvathova E, Sramkova M, Labaj J, Slamenova D (2006) Study of cytotoxic, genotoxic and DNA-protective effects of selected plant essential oils on human cells cultured *in vitro*. Neuroendocrinol Lett 27(Suppl 2):44–47

Horvathova E, Turcaniova V, Slamenova D (2007) Comparative study of DNA-damaging and DNA-protective effects of selected components of essential plant oils in human leukemic cells K562. Neoplasma 54:478–483

Hossain F, Follett P, Salmieri S, Vu KD, Fraschini C, Lacroix M (2019) Antifungal activities of combined treatments of irradiation and essential oils (EOs) encapsulated chitosan nanocomposite films in *in vitro* and in situ conditions. Int J Food Microbiol 295:33–40

Ifeanyichukwu UL, Fayemi OE, Ateba CN (2020) Green synthesis of zinc oxide nanoparticles from pomegranate (*Punica granatum*) extracts and characterization of their antibacterial activity. Molecules. 25(19):4521. https://doi.org/10.3390/molecules25194521

Jiang J, Pi J, Cai J (2018) The advancing of zinc oxide nanoparticles for biomedical applications. Bioinorg Chem Appl 2018:1062562, 18 pages. https://doi.org/10.1155/2018/1062562

John S, Marpu S, Li J, Omary M, Hu Z, Fujita Y, Neogi A (2010) Hybrid zinc oxide nanoparticles for biophotonics. J Nanosci Nanotechnol 10:1707–1712

Kamal E, Kaddam LA, Dahawi M, Osman DM, Salih AM, Alagib A, Saeed A (2018) Gum arabic fibers decreased inflammatory markers and disease severity score among rheumatoid arthritis patients, phase II Trial. Int J Rheumatol 2018:4197537: 6 pages. https://doi.org/10.1155/2018/4197537

Kang SH, Kwon JY, Lee JK, Seo YR (2013) Recent advances in *in vivo* genotoxicity testing: prediction of carcinogenic potential using comet and micronucleus assay in animal models. J Cancer Prev 18:277–288

Kasamoto S, Masumori S, Tanaka J, Ueda M, Fukumuro M, Nagai M, Yamate J, Hayashi M (2017) Reference control data obtained from an *in vivo* comet-micronucleus combination assay using Sprague Dawley rats. Exp Toxicol Pathol 69:187–191

Kasibhatla S, Amarante-Mendes GP, Finucane D, Brunner T, Bossy-Wetzel E, Green DR (2006) Acridine orange/ethidium bromide (AO/EB) staining to detect apoptosis. CSH Protoc 1(3):2006. https://doi.org/10.1101/pdb.prot4493

Kennedy L, Sandhu JK, Harper ME, Cuperlovic-Culf M (2020) Role of glutathione in cancer: from mechanisms to therapies. Biomolecules. 10(10):1429. https://doi.org/10.3390/biom10101429

Kerasioti E, Stagos D, Tsatsakis AM, Spandidos DA, Taitzoglou I, Kouretas D (2018) Effects of sheep/goat whey protein dietary supplementation on the redox status of rats. Mol Med Rep 17(4):5774–5781

Khafaji SSO (2018) Subject review: pharmacological application of thyme. Adv Anim Vet Sci 6(9):366–371

Khalid A, Khan R, Ul-Islam M, Khan T, Wahid F (2017) Bacterial cellulose-zinc oxide nanocomposites as a novel dressing system for burn wounds. Carbohydr Polym 164:214–221

Khorsandi L, Mansouri E, Orazizadeh M, Jozi Z (2016) Curcumin attenuates hepatotoxicity induced by zinc oxide nanoparticles in rats. Balkan Med J 33(3):252–257

Kong H, Yang J, Zhang Y, Fang Y, Nishinari K, Phillips GO (2014) Synthesis and antioxidant properties of gum arabic- stabilized selenium nanoparticles. Int J Biol Macromol 65:155–162

Krol A, Pomastowski P, Rafinska K, Railean-Plugaru V, Buszewski B (2017) Zinc oxide nanoparticles: synthesis, antiseptic activity and toxicity mechanism. Adv Colloid Interf Sci 249:37–52

Kumar B, Smita K, Cumbal L, Alexis Debut A (2014) Green approach for fabrication and applications of zinc oxide nanoparticles. Bioinorg Chem Appl 2014:523869, 7 pages. https://doi.org/10.1155/2014/523869

Kumaravel TS, Vilhar B, Faux SP, Jha AN (2009) Comet assay measurements: a perspective. Cell Biol Toxicol 25:53–64

Kuznetsov AV, Javadov S, Grimm M, Margreiter R, Ausserlechner MJ, Hagenbuchner J (2020) Crosstalk between mitochondria and cytoskeleton in cardiac cells. Cells 9(1):222. https://doi.org/10.3390/cells9010222

Lakshmi SJ, Roopa Bai RS, Sharanagouda H, Ramachandra CT, Sharanagouda H, Nadagouda S, Doddagoudar SR (2017) Biosynthesis and characterization of ZnO nanoparticles from spinach (*Spinacia oleracea*) leaves and its effect on seed quality parameters of greengram (*Vigna radiata*). Int J Curr Microbiol App Sci 6:3376–3384

Lee KW, Everts H, Beynen AC (2004) Essential oils in broiler nutrition. Int Poult Sci 3:738–752

Li CH, Shen CC, Cheng YW, Huang SH, Wu CC, Kao CC, Liao JW, Kang JJ (2012) Organ biodistribution, clearance, and genotoxicity of orally administered zinc oxide nanoparticles in mice. Nanotoxicol. 6:746–756

Li HF, Ding F, Xiao LY, Shi RN, Wang HY, Han WJ (2017) Food-derived antioxidant polysaccharides and their pharmacological

potential in neurodegenerative diseases. Nutrients 9:778. https://doi.org/10.3390/md17120674

Lin CC, Hsu YF, Lin TC, Hsu FL, Hsu HY (1998) Antioxidant and hepatoprotective activity of Punicalagin and Punicalin on carbon tetrachloride induced liver damage in rats. J Pharm Pharmacol 50: 789–794

Mahamuni PP, Patil PM, Dhanavade MJ, Badiger MV, Shadija PG, Lokhande AC, Bohara RA (2019) Synthesis and characterization of zinc oxide nanoparticles by using polyol chemistry for their antimicrobial and antibiofilm activity. Biochem Biophys Rep 17:71–80

Maisanaba S, Prieto AI, Puerto M, Gutierrez-Praena D, Demir E, Marcos R, Camean AM (2015) *In vitro* genotoxicity testing of carvacrol and thymol using the micronucleus and mouse lymphoma assays. Mutat Res Genet Toxicol Environ Mutagen 784-785:37–44

Mirghani MES, Elnour AAM, Kabbashi NA, Alam MZ, Musa KH, Abdullah A (2018) Determination of antioxidant activity of gum Arabic: an exudation from two different locations. Sci Asia 44(2018):179–186

Moatamed ER, Hussein AA, El-Desoky MM, Khayat Z (2019) Comparative study of zinc oxide nanoparticles and its bulk form on liver function of Wistar rat. Toxicol Ind Health 35(10):627–637

Mohammad GRKS, Seyedi SMR, Karimi E, Homayouni-Tabrizi M (2019) The cytotoxic properties of zinc oxide nanoparticles on the rat liver and spleen, and its anticancer impacts on human liver cancer cell lines. J Biochem Mol Toxicol 33(7):e22324. https://doi.org/10.1002/jbt.22324

Mohammed KAA, Ahmed HMS, Sharaf HA, El-Nekeety AA, Abdel-Aziem SH, Mehaya FM, Abdel-Wahhab MA (2020) Encapsulation of cinnamon oil in whey protein counteracts the disturbances in gene expression and diabetic complications in rats. Environ Sci Pollut Res Int 27:2829–2843

Moras M, Lefevre SD, Ostuni MA (2017) From erythroblasts to mature red blood cells: organelle clearance in mammals. Front Physiol 8: 1076. https://doi.org/10.3389/fphys.2017.01076

Mudunkotuwa IA, Rupasinghe T, Wu CM, Grassian VH (2012) Dissolution of ZnO nanoparticles at circumneutral pH: a study of size effects in the presence and absence of citric acid. Langmuir 28: 396–403

Müller P, Schmid M (2019) Intelligent Packaging in the food sector: a brief overview. Foods 8(1):16. https://doi.org/10.3390/foods8010016

Pati R, Das I, Mehta RK, Sahu R, Sonawane A (2016) Zinc-oxide nanoparticles exhibit genotoxic, clastogenic, cytotoxic and actin depolymerization effects by inducing oxidative stress responses in macrophages and adult mice. Toxicol Sci 150:454–472

Pecarski D, Knežević-Jugović Z, Dimitrijević-Branković S, Mihajilovski K, Janković S (2014) Preparation, characterization and antimicrobial activity of chitosan microparticles with thyme essential oil. Hem Ind 68(6):721–729

Pourmirzaiee MA, Chehrazi S, Heidari-Beni M, Kelishadi R (2018) Serum zinc level and eating behaviors in children receiving zinc supplements without physician prescription. Adv Biomed Res 7: 120. https://doi.org/10.4103/abr.abr_77_18 eCollection 2018

Prasad AS (2008) Clinical, immunological, anti-inflammatory and antioxidant roles of zinc. Exp Gerontol 43(5):370–377

Rašković A, Pavlović N, Kvrgić M, Sudji J, Mitić G, Čapo I, Mikov M (2015) Effects of pharmaceutical formulations containing thyme on carbon tetrachloride-induced liver injury in rats. BMC Complement Altern Med 15:442. https://doi.org/10.1186/s12906-015-0966-z

Rasmussen JW, Martinez E, Louka P, Wingett DG (2010) Zinc oxide nanoparticles for selective destruction of tumor cells and potential for drug delivery applications. Expert Opin Drug Deliv 7:1063–1077

Razzaghi-Abyaneh M, Shams-Ghahfarokhi M, Rezaee M, Jaimand K, Alinezhad S, Saberi R, Yoshinar T (2009) Chemical composition and antiaflatoxigenic activity of *Carum carvi* L., *Thymus vulgaris* and *Citrus aurantifolia* essential oils. Food Control 20:1018–1024

Reis Éde M, de Rezende AA, Santos DV, de Oliveria PF, Nicolella HD, Tavares DC, Silva AC, Dantas NO, Spanó MA (2015) Assessment of the genotoxic potential of two zinc oxide sources (amorphous and nanoparticles) using the *in vitro* micronucleus test and the *in vivo* wing somatic mutation and recombination test. Food Chem Toxicol 84:55–63

Rodzik A, Pomastowski P, Sagandykova GN, Buszewski B (2020) Interactions of whey proteins with metal ions. Int J Mol Sci 21(6): 2156. https://doi.org/10.3390/ijms21062156

Rojas-Armas J, Arroyo-Acevedo J, Ortiz-Sánchez M, Palomino-Pacheco M, Castro-Luna A, Ramos-Cevallos N, Justil-Guerrero H, Hilario-Vargas J, Herrera-Calderón O (2019) Acute and repeated 28-day oral dose toxicity studies of *Thymus vulgaris L.* essential oil in rats. Toxicol Res 35:225–232

Rota MCA, Herrera RM, Martinez JA, Sotomayor M, Jordan MJ (2007) Antimicrobial activity and chemical composition of *Thymus vulgaris, Thymus zygis* and *Thymus hyemalisessential* oils. Food Control 19:681–687

Sahu N, Saxena J (2013) Different methods for determining antioxidant activity: a review. Indo Am J Pharma Res 3:7025–7028

Saliani M, Jalal R, Goharshadi EK (2016) Mechanism of oxidative stress involved in the toxicity of ZnO nanoparticles against eukaryotic cells. Nanomed J 3(1):1–14

Sha B, Gao W, Wang S, Gou X, Li W, Liang X, Qu Z, Xu F, Lu TJ (2014) Oxidative stress increased hepatotoxicity induced by nano-titanium dioxide in BRL-3A cells and Sprague-Dawley rats. J Appl Toxicol 34(4):345–356

Shaban EE, Elbakry HFH, Ibrahim KS, El Sayed EM, Salama DM, Farrag AH (2019) The effect of white kidney bean fertilized with nano-zinc on nutritional and biochemical aspects in rats. Biotechnol Rep (Amst) 23:e00357. https://doi.org/10.1016/j.btre

Shalini D, Senthilkumar S, Rajaguru P (2018) Effect of size and shape on toxicity of zinc oxide (ZnO) nanomaterials in human peripheral blood lymphocytes. Toxicol Mech Methods 28:87–94

Sharma V, Anderson D, Dhawan A (2011) Zinc oxide nanoparticles induce oxidative stress and genotoxicity in human liver cells (HepG2). J Biomed Nanotechnol 7:98–99

Sharma V, Anderson D, Dhawan A (2012) Zinc oxide nanoparticles induce oxidative DNA damage and ROS-triggered mitochondria mediated apoptosis in human liver cells (HepG2). Apoptosis 17(8):852–870

Singh S (2019) Zinc oxide nanoparticles impacts: cytotoxicity, genotoxicity, developmental toxicity, and neurotoxicity. Toxicol. Mech Methods 29:300–311

Smart DJ, Helbling FR, Verardo M, McHugh D, Vanscheeuwijck P (2019) Mode-of-action analysis of the effects induced by nicotine in the *in vitro* micronucleus assay. Environ Mol Mutagen 60(9): 778–791

Soni D, Gandhi D, Tarale P, Bafana A, Pandey RA, Sivanesan S (2017) Oxidative stress and genotoxicity of zinc oxide nanoparticles to Pseudomonas species, human promyelocytic leukemic (HL-60), and blood cells. Biol Trace Elem Res 178:218–227

Srivastav AK, Kumar M, Ansari NG, Jain AK, Shankar J, Arjaria N, Jagdale P, Singh D (2016) A comprehensive toxicity study of zinc oxide nanoparticles versus their bulk in Wistar rats: toxicity study of zinc oxide nanoparticles. Hum Exp Toxicol 35(12):1286–1304

Stan M, Popa A, Toloman D, Silipas T, Vodnar DC, Katona G (2015) Enhanced antibacterial activity of zinc oxide nanoparticles synthesized using *Petroselinum crispum* extracts. AIP Conf Proceed 1700: 060004. https://doi.org/10.1063/1.4938454

Syama S, Sreekanth PJ, Varma HK, Mohanan PV (2014) Zinc oxide nanoparticles induced oxidative stress in mouse bone marrow mesenchymal stem cells. Toxicol Mech Methods 24:644–653

Tang HQ, Xu M, Rong Q, Jin RW, Liu QJ, Li YL (2016) The effect of ZnO nanoparticles on liver function in rats. Int J Nanomedicine 11: 4275–4285

Tian L, Lin B, Lei WL, Li K, Liu H, Yan J, Liu X, Zhuge X (2015) Neurotoxicity induced by zinc oxide nanoparticles: age-related differences and interaction. Sci Rep 5:16117. https://doi.org/10.1038/srep16117

Tomazelli Júnior O, Kuhn F, Padilha PJM, Vicente LRM, Costa SW, Boligon AA, Scapinellob J, Nesi CN, Dal Magrob J, Lamo Castellví S (2018) Microencapsulation of essential thyme oil by spray drying and its antimicrobial evaluation against *Vibrio alginolyticus* and *Vibrio parahaemolyticus*. Braz J Biol 78(2):311–317

Toujani MM, Rittà M, Civra A, Genovese S, Epifano F, Ghram A, Lembo D, Donalisio M (2018) Inhibition of HSV-2 infection by pure compounds from Thymus capitatus extract *in vitro*. Phytother Res 32(8):1555–1563

Turkez H, Aydin E (2016) Investigation of cytotoxic, genotoxic and oxidative properties of carvacrol in human blood cells. Toxicol Ind Health 32:625–633

Ündeğer U, Basaran A, Degen GH, Basaran N (2009) Antioxidant activities of major thyme ingredients and lack of (oxidative) DNA damage in V79 Chinese hamster lung fibroblast cells at low levels of carvacrol and thymol. Food Chem Toxicol 47:2037–2043

Ushida K, Hatanaka H, Inoue R, Tsukahara T, Phillips GO (2011) Effect of long-term ingestion of gum arabic on the adipose tissues of female mice. Food Hydrocoll 25(5):1344–1349

Wang B, Feng W, Wang M, Wang T, Gu Y, Zhu M, Ouyang H, Shi J, Zhang F, Zhao Y, Chai Z, Wang H, Wang J (2008) Acute toxicological impact of nano- and submicro-scaled zinc oxide powder on healthy adult mice. J Nanopart Res 10:263–276

Wang B, Fenga WY, Wang TC, Jia G, Wang M, Shi JW, Zhang F, Zhao YL, Chai ZF (2006) Acute toxicity of nano- and micro-scale zinc powder in healthy adult mice. Toxicol Lett 161:115–123

Wang B, Zhang J, Chen C, Xu G, Qin X, Hong Y, Bose DD, Qiu F, Zou Z (2018) The size of zinc oxide nanoparticles controls its toxicity through impairing autophagic flux in A549 lung epithelial cells. Toxicol Lett 285:51–59

Wang B, Zhang Y, Mao Z, Yu D, Gao C (2014) Toxicity of ZnO nanoparticles to macrophages due to cell uptake and intracellular release of zinc ions. J Nanosci Nanotechnol 14:5688–5696

Wang JQ, Hu SZ, Nie SP, Yu Q, Xie MY (2016) Reviews on mechanisms of *in vitro* antioxidant activity of polysaccharides. Oxidative Med Cell Longev 2016:5692852. https://doi.org/10.1155/2016/5692852

Wang M, Wang J, Liu Y, Wang J, Nie Y, Si B, Liu Y, Wang X, Chen S, Hei TK, Wu L, Zhao G, Xu A (2019) Subcellular targets of zinc oxide nanoparticles during the aging process: role of cross-talk between mitochondrial dysfunction and endoplasmic reticulum stress in the genotoxic response. Toxicol Sci 171:159–171. https://doi.org/10.1093/toxsci/kfz132

Wang Y, Yuan L, Yao C, Ding L, Li C, Fang J, Sui K, Liu Y, Wu M (2014a) A combined toxicity study of zinc oxide nanoparticles and vitamin C in food additives. Nanoscale 6(24):15333–15342

Wang ZJ, Xie J, Nie SP, Xie MY (2017) Review on cell models to evaluate potential antioxidant activity of polysaccharides. Food Funct 8:915–926

Wessels I, Rolles B, Rink L (2020) The potential impact of zinc supplementation on COVID-19 pathogenesis. Front Immunol 11:1712. https://doi.org/10.3389/fimmu.2020.01712

Wu B, Wang Y, Lee YH, Horst A, Wang Z, Chen DR, Sureshkumar R, Tang YJ (2010) Comparative eco-toxicities of nano-ZnO particles under aquatic and aerosol exposure modes. Environ Sci Technol 44(4):1484–1489

Yan Y, Wang G, Huang J, Zhang Y, Cheng X, Chuai M, Brand-Saberi B, Chen G, Jiang X, Yang X (2020) Zinc oxide nanoparticles exposure-induced oxidative stress restricts cranial neural crest development during chicken embryogenesis. Ecotoxicol Environ Saf 194:110415. https://doi.org/10.1016/j.ecoenv.2020.110415

Yousef MI, Mutar TF, Kamel MAE (2019) Hepato-renal toxicity of oral sub-chronic exposure to aluminum oxide and/or zinc oxide nanoparticles in rats. Toxicol Rep 6:336–346

Zahin N, Anwar R, Tewari D, Kabir MT, Sajid A, Mathew B, Uddin MS, Aleya L, Abdel-Daim MM (2020) Nanoparticles and its biomedical applications in health and diseases: special focus on drug delivery. Environ Sci Pollut Res Int 27(16):19151–19168

Zarria-Romero J, Osorio A, Pino J, Shiga B, Vivas-Ruiz D (2017) Effect of the industrial nanoparticles TiO_2 , SiO_2 and ZnO on cell viability and gene expression in red bone marrow of *Mus Musculus*. Rev Peru Med Exp Salud Publica 34:436–444

Zhong Q, Wei B, Wang S, Ke S, Chen J, Zhang H, Wang H (2019) The antioxidant activity of polysaccharides derived from marine organisms: an overview. Mar Drugs 17(12):674. https://doi.org/10.3390/md17120674